RSC Medicinal Chemistry

ROYAL SOCIETY OF CHEMISTRY

REVIEW

View Article Online
View Journal

Cite this: DOI: 10.1039/d6md00119j

Targeting DNA-PK: medicinal chemistry insights into small-molecule inhibitor discovery and optimisation

Elle Watson, [a] Jack R. R. Hutchinson, [a] Suzannah J. Harnor, [a] Luke Gaughan[b] and Celine Cano *[a]

DNA-dependent protein kinase (DNA-PK) is a central regulator of non-homologous end joining (NHEJ), the dominant pathway for DNA double-strand break repair in mammalian cells. Aberrant DNA-PK activity is frequently associated with tumour progression as well as chemo- and radio-resistance, positioning DNA-PK as an attractive therapeutic target in cancer. Over the past few years, extensive medicinal chemistry efforts have enabled the optimisation of small molecule inhibitors of DNA-PK, from early, non-selective chemical probes into highly potent, selective and orally bioavailable compounds. This review provides a comprehensive overview of the discovery and optimisation of DNA-PK inhibitors, highlighting key structure–activity relationships, synthetic strategies and pharmacological profiles across several inhibitor generations. Representative scaffolds, including chromen-4-one derivatives and next-generation clinical candidates such as AZD7648 and VX-984, are discussed. Finally, we summarise current clinical progress in early phase trials and remaining challenges, including achieving tolerability and efficacy when compounds are administered both as a single agent, or in combination. Taken together, this review highlights both the therapeutic potential of DNA-PK-targeting inhibition and the challenges encountered in clinical development, providing a framework to guide future strategies for DNA-PK-targeted therapeutics.

Received 13th February 2026,
Accepted 24th May 2026

DOI: 10.1039/d6md00119j

rsc.li/medchem

Introduction

DNA double-strand breaks (DSBs) are induced by both intrinsic and extrinsic stimuli, and result in genomic instability, which is a hallmark of cancer development.[1] These DSBs can be repaired *via* homologous recombination (HR) in the S and G2 phases of the cell cycle, or non-homologous end joining (NHEJ) across the cell cycle.[2–4] DNA-dependent kinase (DNA-PK) is a serine/threonine protein

[a] *Cancer Research Horizons Newcastle Drug Discovery Unit, Chemistry, School of Natural and Environmental Sciences, Newcastle University, Bedson Building, Newcastle upon Tyne, NE1 7RU, UK. E-mail: celine.cano@newcastle.ac.uk*
[b] *Newcastle University Centre for Cancer, Paul O'Gorman Building, Framlington Place, Newcastle upon Tyne, NE2 4HH, UK*

Elle Watson

Elle Watson is currently a 3rd year PhD researcher at the Drug Discovery Unit in the Newcastle University Cancer Research Centre. She received her master's degree in chemistry with Medicinal Chemistry from Newcastle University in 2023. Her current research focuses on developing new modalities in DNA repair.

Jack Hutchinson

Jack Hutchinson received a first-class MChem degree from Newcastle University in 2024, where he completed his final year project under the supervision of Dr Celine Cano. He continued at Newcastle University and is now a second-year PhD student in Dr Cano's group. His research focuses on the design and development of new modalities in DNA repair.

kinase which plays a crucial role in the repair of DSBs *via* the NHEJ pathway.[5] The holoenzyme is composed of a catalytic subunit, DNA-PK$_{cs}$, and a heterodimeric regulatory factor, Ku70/Ku80.[5] The Ku heterodimer detects DSBs and threads onto each damaged DNA end, changing the confirmation of the Ku subunit and forming a Ku–DNA complex, which stabilises the DNA ends and prevents nucleolytic degradation.[4–7] The DNA-PK$_{cs}$, in complex with Artemis, has a high affinity for the Ku–DNA ends, and thus it binds to Ku, forming the active DNA-PK complex. Recent structural and biochemical studies have elaborated on the dynamics of DNA-PK, establishing it as more than just a catalytic entity. High-resolution structural analyses demonstrate that DNA-PK is composed of multiple HEAT repeats which facilitates the formation of synaptic complexes.[6,8] Long-range synapsis occurs when the DNA-PK$_{cs}$ complexes on each DSB end dimerise, bringing the two strands of DNA closer together, forming a weak complex. DNA-PK$_{cs}$ then undergoes autophosphorylation in the ABCDE cluster, which causes a substantial conformational change.[9,10] This process causes DNA-PK$_{cs}$ to dissociate from the Ku–DNA complex, while Artemis is activated by DNA-PK$_{cs}$, thus beginning the DNA end processing.[4,11] Other nucleases may be recruited, but Artemis is often the primary one, resecting the DNA ends *via* its endonuclease activity. In addition, DNA polymerases μ and λ (Pol μ and Pol λ, respectively) can then incorporate deoxynucleoside triphosphates (dNTPs) to bridge the gap between the strands, making them compatible for ligation. Finally, DNA ligase IV, in association with X-ray cross-complementing protein 4 (XRCC4), facilitates the final ligation between DNA ends, now closer together as part of a short-range synaptic complex. XRCC4-like factor (XLF) interacts with XRCC4 and the XRCC4-XLF complex is believed to form a sleeve around the DNA duplex, stabilising the ends before covalent ligation.[7] Once the two strands have been ligated, the DNA-PK complex dissociates.

DNA-PK is also essential for the repair of RAG-induced DSBs during *V*(*D*)*J* recombination, a strictly regulated series of DNA breakage and rejoining events that generate antigen receptor diversity through the assembly of variable (*V*), diversity (*D*) and joining (*J*) gene segments. Although this is a preprogrammed genetic rearrangement, rather than canonical DDR, it co-opts DDR machinery, including DNA-PK and its associated NHEJ factors. This positions DNA-PK as a key mediator of lymphocyte development, specifically in the assembly of immunoglobulin and T-cell receptor genes.[12–14]

Notwithstanding the strong association of DNA-PK$_{cs}$ function with the DDR *via* the NHEJ pathway, it was first characterised several decades ago as a transcriptional regulator of the transcription factor SP1; a process involving DNA-dependent DNA-PK-mediated SP1 phosphorylation.[15] Since then, multiple transcription factors across a range of families, including androgen receptor (AR), HIF-1 and ERG,

Suzannah Harnor

Suzannah Harnor received her BSc and MRes from the University of Dundee and completed her PhD in natural product chemistry at the University of Glasgow. She is currently a Senior Research Associate in medicinal chemistry at Newcastle University. Her research focuses on the design and synthesis of small molecules for therapeutic applications, integrating structure-based drug design with synthetic methodologies to address key challenges in drug discovery.

Luke Gaughan

Luke Gaughan completed his PhD in molecular biology in 2001 and is now a Reader/ Associate Professor of molecular oncology in the Newcastle University Centre for Cancer. His research focuses on androgen receptor signalling, pathogenic splicing and DNA repair in prostate cancer.

Celine Cano

Celine Cano received her PhD on carbohydrate chemistry from the University of Poitiers, France, in 2004. After postdoctoral research at the University of Manchester with Prof. John A. Joule where she worked on oxomolybdoenzyme cofactor analogues, she joined Newcastle University as a Cancer Research UK research fellow in 2005. She is currently a Reader (Associate Professor) in Medicinal Chemistry, where her research focuses on small-molecule anticancer agents. In 2017, she received the Elsevier Reaxys Prize for Medicinal Chemistry in recognition of her research in DNA repair.

have been shown to be dependent on DNA-PK$_{cs}$ for controlling transcriptional competency.[16,17] More recently, the discovery that DNA-PK$_{cs}$ controls: (i) splicing; (ii) innate and adaptive immune responses, in part by regulating cGAS signalling and T cell proliferation, respectively; and (iii) metabolic activity has established the enzyme as a key node of pleiotropic cellular regulation.[18–22]

Aberrant expression and dysregulation of DNA-PK have been increasingly implicated in cancer development, progression and resistance to treatment. Elevated levels of DNA-PK$_{cs}$ have been reported in multiple malignancies, including breast, prostate, lung, ovarian and hepatocellular carcinomas and frequently correlate with poor prognosis and survival.[23–25] Overexpression of DNA-PK enhances the repair of therapy-induced DNA damage, conferring resistance to ionising radiation (IR) and genotoxic chemotherapies, such as traditional cisplatin and doxorubicin treatment.[23–26] In certain cancers, DNA-PK$_{cs}$ has also been shown to promote metastatic behaviour through involvement in cell proliferation.[27]

Since the elucidation of the role of DNA-PK overexpression in treatment resistance, numerous DNA-PK$_{cs}$ inhibitors have been developed. This review will summarise key developments, medicinal chemistry optimisation, representative syntheses and clinical development, with a particular focus on the most recent advances. A comparative summary of their mechanisms, activity and key strengths and limitations is provided in Tables 1 and 2.

Evolution of small-molecule inhibitors

Early DNA-PK inhibitors have progressively shaped the medicinal chemistry landscape from early non-selective, covalent PI3K inhibitors to potent, drug-like and more selective compounds. Each structural evolution improved potency, selectivity and pharmacokinetic performance, supporting the potential of DNA-PK inhibition in cancer therapy (Fig. 1).

Table 1 Comparative overview of DNA-PK inhibitors

Inhibitor	Type/mechanism	DNA-PK IC_{50}	Selectivity[a]	Key features/limitations
Wortmannin	Irreversible covalent	16 nM	Non-selective (pan PIKK)	First PIKK inhibitor; radiosensitiser; poor drug-like properties, toxicity
KU-0060648	Reversible, dual DNA-PK/PI3K ATP-competitive	5 nM	Moderate	Potent, improved PK, strong chemo-/radiosensitiser
Phenol IC series (*e.g.* IC60211)	Reversible ATP-competitive	0.4 μM to nM (400 nM)	High (*vs.* PI3Kβ)	Low toxicity, synergistic with DNA-damaging agents
Vanillin (*e.g.* 4,5-dimethoxy-2-nitrobenzaldehyde)	Irreversible covalent	1.5 mM (15 μM)	Low	Low potency but simple scaffold useful for covalent design
SU11752	Reversible ATP-competitive	0.13 μM	Moderate	Low potency; poor pharmacokinetics; unsuitable for *in vivo* use
LY294002	Reversible ATP-competitive	1.5 μM	Low	Low potency; poor *in vivo* stability, *in vivo* toxicity, high clearance
NU7026	Reversible ATP-competitive	0.23 μM	Moderate	Low potency; poor pharmacokinetics; unsuitable for clinical use
NU7441	Reversible ATP-competitive	14 nM	High (*vs.* class I PI3Ks)	High potency; low aqueous solubility and poor oral bioavailability
NU5455	Reversible ATP-competitive	8.2 nM	High (*vs.* class I PI3Ks)	High potency; effective radiosensitiser *in vitro* and *in vivo*; lack of clinical application
CC-115	Reversible ATP-competitive	13 nM	Moderate	High potency; limited clinical efficacy; toxicity
M3814	Reversible ATP-competitive	0.6 nM	High	High potency; strong chemo-/radiosensitiser; clinically advanced; normal cell toxicity observed in trials
VX-894	Reversible ATP-competitive	—	—	Effective radiosensitiser *in vitro* and *in vivo*; preferential activity in tumour cells; lack of medicinal chemistry data; limited clinical progress
D11	Reversible ATP-competitive	10.2 nM	Moderate	High potency; good PK properties; significant inhibition of ATM; breadth of kinase selectivity is unclear
BR101801	Reversible ATP-competitive	15 nM	Low	High potency; promising clinical profile
AZD7648	Reversible ATP-competitive	0.6 nM	High (*vs.* class I PI3Ks)	High potency; limited clinical efficacy; toxicity observed in combination therapy
BAY-8400	Reversible ATP-competitive	81 nM	Low	High potency; antitumour efficacy; low oral bioavailability; low metabolic stability
XRD-0394	Reversible ATP-competitive	0.89 nM	Moderate	High potency; promising clinical profile
DA-143	Reversible ATP-competitive	2.5 nM	Moderate (*vs.* class I PI3Ks)	High potency; improved aqueous solubility; limited pharmacokinetic data

[a] Selectivity categorised as ≤50-fold ~ low, 50–100-fold ~ moderate, ≥100-fold ~ high.

Table 2 Representative selection of leading DNA-PK inhibitors and their respective pharmacokinetic and PK/PD profiles

Parameter	AZD7648 (ref. 76 and 77)	CC-115 (ref. 65–68 and 90)	M3814 (ref. 62)
Biochemical IC_{50} (DNA-PK)	0.6 nM	13 nM	0.6 nM
Cellular IC_{50}	50–100 nM	15 nM to 1.77 μM	ND
Oral bioavailability (*F*%)	104% (rat), 93% (dog)	27% (rat)	~20% (mouse)
C_{max} (clinical)[a]	2463 nmol L^{-1}[b]	~36.1–173 ng mL^{-1}[c]	437 ng mL^{-1}[d]
AUC_{∞} (clinical)[a]	25 180 h × nmol L^{-1}[b]	~237–2130 h × ng mL^{-1}[c]	2390 h × ng mL^{-1}[d]
Half-life ($t_{1/2}$)[a]	10.32 h[b]	~3.98–7.90 h[c]	6.3 h[d]
Clearance[a]	8.353 L h^{-1}[b]	~13.1–33.7 L h^{-1}[c]	41.9 L h^{-1}[d]
Volume of distribution[a]	1.4 L (rat), 0.7 L (dog)	~149–294 L (human)	382 L[d]
PK/PD biomarkers	γH2AX, pDNA-PK_{cs}	γH2AX, mTOR markers	p-DNA-PK_{cs}
PK/PD relationship	Strong, exposure-driven	Dual-pathway complexity	Dose-dependent
Primary clinical strategy	Combination (PLD)	Combination/multitarget	Monotherapy

[a] Results in plasma. [b] Values from BID 80 mg cohort, day 0, cycle 1 (NCT03907969). [c] Values across QD of 8 mg, 16 mg, 25 mg and 40 mg and BID of 10 mg and 15 mg. [d] Values from QD 100 mg cohort, day 1, cycle 1 (NCT02316197).

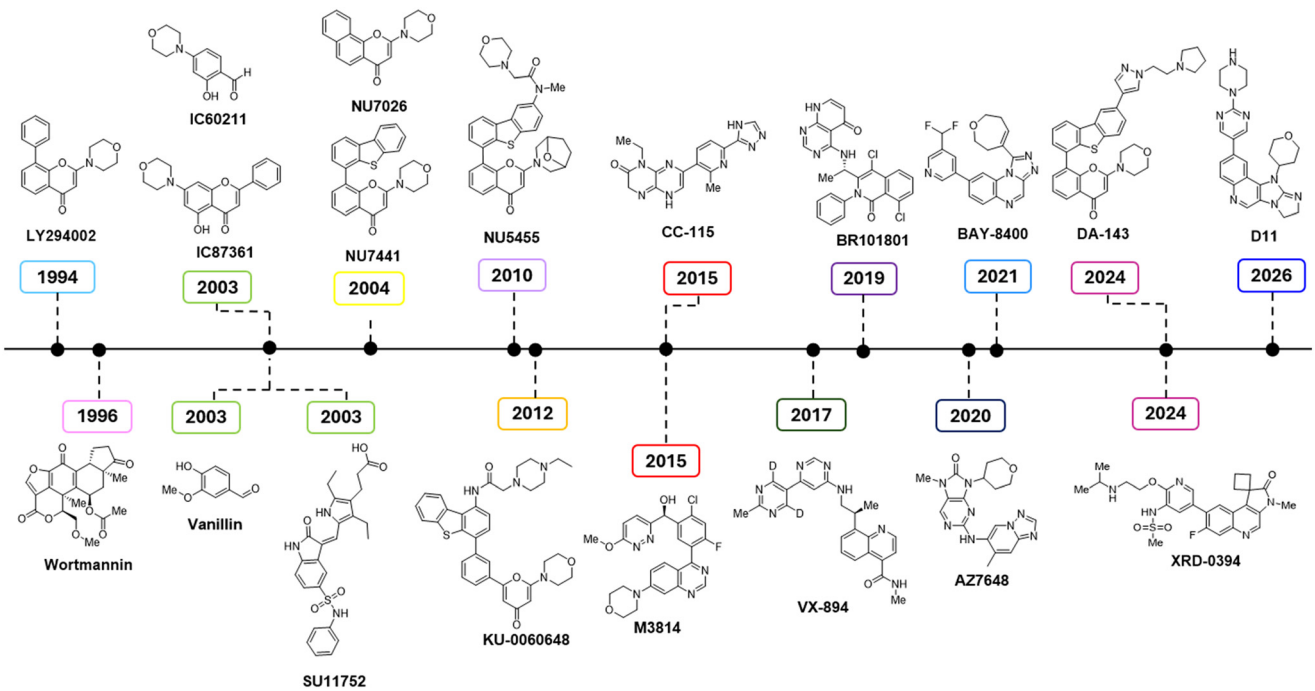

Fig. 1 Timeline of identification of DNA-PK inhibitors.

Compounds such as wortmannin[28–32] and LY294002,[33,34] along with ICOS Corporation's arylmorpholine inhibitors,[35–37] vanillin-based aldehydes[36,37] and tool compounds like SU11752,[38] were instrumental in establishing DNA-PK as a tractable target. These compounds demonstrated that small-molecule inhibition of DNA-PK could impair DNA double-strand break repair and potentiate the effects of ionising radiation and DNA-damaging agents.

However, these early inhibitors were limited by variable potency and poor selectivity across PIKK family members (including PI3K, ATM, ATR and mTOR). In addition, several scaffolds suffered from poor physicochemical and pharmacokinetic properties, including low metabolic stability, high clearance and off-target reactivity. Irreversible or reactive chemotypes (*e.g.*, wortmannin and aldehyde derivatives) further limited their suitability for drug development. Consequently, these compounds have largely been confined to use as biochemical and cellular tool molecules. Comprehensive accounts of these early inhibitors are provided in earlier review articles (*e.g.* Cano *et al.*, 2018).[39]

The development of more selective and drug-like DNA-PK inhibitors was enabled by advances in structure-based drug design (SBDD) and better understanding of kinase active-site interactions. Early scaffolds, particularly the chromen-4-one core, provided critical structure–activity relationship (SAR) insights, with the morpholine substituent highlighting key interactions within the ATP-binding pocket that informed subsequent optimisation strategies. These findings established a foundation for the rational design of more potent and selective analogues. The emergence of the NU

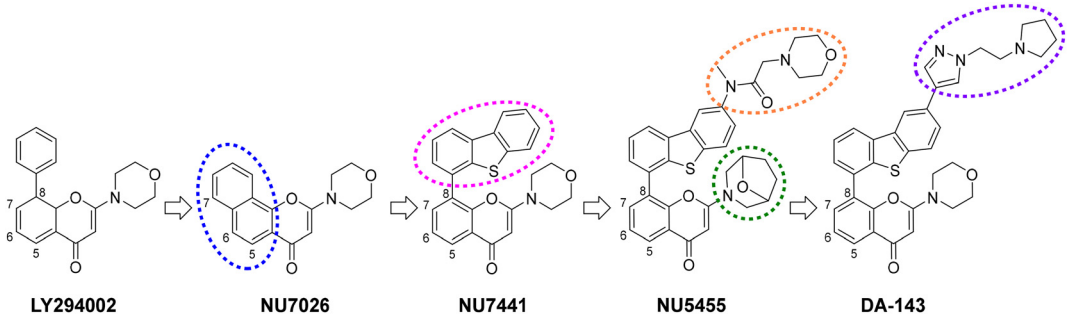

Fig. 2 Development of chromen-4-one DNA-PK inhibitors. Each new motif highlighted by colour.

series marked a key point in DNA-PK inhibitor development, as these compounds exhibit substantially improved potency, selectivity and pharmacokinetic properties (Fig. 2).

Chromen-4-one-based inhibitors and the emergence of NU5455

LY294002. In 1994, Lilly Pharmaceuticals identified LY294002,[33] a reversible PI3K inhibitor with a chromen-4-one (flavonoid-like) scaffold and an essential morpholine ring that hydrogen bonds to Val882 within the ATP-binding pocket of PI3Kγ.[31] Although LY294002 inhibited DNA-PK with an IC_{50} of ~1.5 μM, it lacked selectivity, had poor *in vivo* stability as well as *in vivo* toxicity and high clearance.[33,34]

NU7026. Medicinal chemistry efforts at Newcastle University and KuDOS Pharmaceuticals generated an optimised series of benzopyranones and pyrimidoisoquinolinone derivatives.[34] Griffin *et al.* synthesised NU7026 which retained the necessary morpholine and introduced a fused biaryl system (Fig. 2, highlighted in blue) on the chromen-4-one scaffold. NU7026 demonstrated a 56-fold selectivity for DNA-PK over PI3K family members and a promising IC_{50} of 0.23 μM. Several human tumour cell lines were treated with NU7026 *in vitro* which showed the inhibitor to act as both a radio- and chemo-sensitiser.[40,41]

NU7441. With the goal of enhancing activity, functionality was introduced on the 6-, 7- and 8-position of the chromen-4-one core as this was known to be tolerated at the ATP-binding domain of DNA-PK.[42] As a result, NU7441 was successfully identified with an IC_{50} of 14 nM and the significant improvement in potency was attributed to the dibenzothiophen-1-yl group (Fig. 2, highligted in pink). Selectivity for DNA-PK increased to 360-fold over PI3K family members. Key binding interactions were elucidated by Blundell *et al.* of NU7441 bound to $DNA\text{-}PK_{cs}$, highlighting hydrogen bonding interactions between the chromen-1-one core and morpholine ring to the peptide backbones of Asp3941 and Leu3806.[43] Additional binding interactions were shown between the dibenzothiophene group and the N-lobe, where it docks in the hydrophobic groove of Met3729, Pro3735 and Leu3751.

The therapeutic potential of NU7441 was further explored across multiple human tumour cell lines including breast, prostate and colon cancer and demonstrated its capability as a radiosensitiser and chemosensitiser.[44–46] Moreover, in prostate cancer cell lines and xenografts, transcriptional activity of both the AR and pathogenic androgen–receptor splice variants, which are refractory to current AR-targeting agents, significantly reduced upon treatment with NU7441 (the latter observation also replicated with AZD7648 and NU5455; see below), which translated to diminished tumour cell proliferation *in vitro* and *in vivo*; highlighting the benefit of targeting the transcriptional co-regulatory role of DNA-PK for cancer treatment.[24,47]

Consistent with the role of DNA-PK negatively regulating innate immune responses *via* the cGAS pathway, which is a critical node of interferon-driven inflammatory signalling and key for priming of cytotoxic T-cells, NU7441 was shown to abolish repressive DNA-PK-mediated cGAS phosphorylation to enhance cGAS activity and downstream inflammatory signalling.[21] This phenomenon has been demonstrated to be critical for the cytotoxic effects of combined doxorubicin and DNA-PKIs in multiple myeloma models and offers new opportunities for immunotherapy considerations in future pre-clinical and clinical studies.

Unfortunately, clinical applications of NU7441 are limited due to poor aqueous solubility and oral bioavailability.

NU5455. In 2011, the NU series was further developed with the intention of improving pharmacokinetic properties. Replacement of the necessary morpholine for 8-oxa-3-azabicyclo[3.2.1]octane (Fig. 2, highlighted in green) as well as addition of amide linked morpholine at the 2-poisition of the dibenzothiophene motif (Fig. 2, highlighted in orange). Structural changes were not only tolerated but afforded NU5455 with an improved IC_{50} of 8.2 nM and improved solubility, whilst retaining high selectivity against PI3K family members.

The synthetic route for NU5455 follows similar chemistry to the previous chromen-4-one series, including the final Suzuki–Miyaura coupling (Scheme 1). The overall synthesis is 11-steps, beginning with the acetylation of 8-oxa-3-azabicyclo[3.2.1]octane (**1**) to form the corresponding amide **2** and the formation of chromen-4-one **4** follows established chemistry. More interesting is the synthesis of intermediate **10** which begins with conversion of 2-bromo-2-methylpropanoyl bromide to the corresponding amide, followed by an S_NAr reaction with

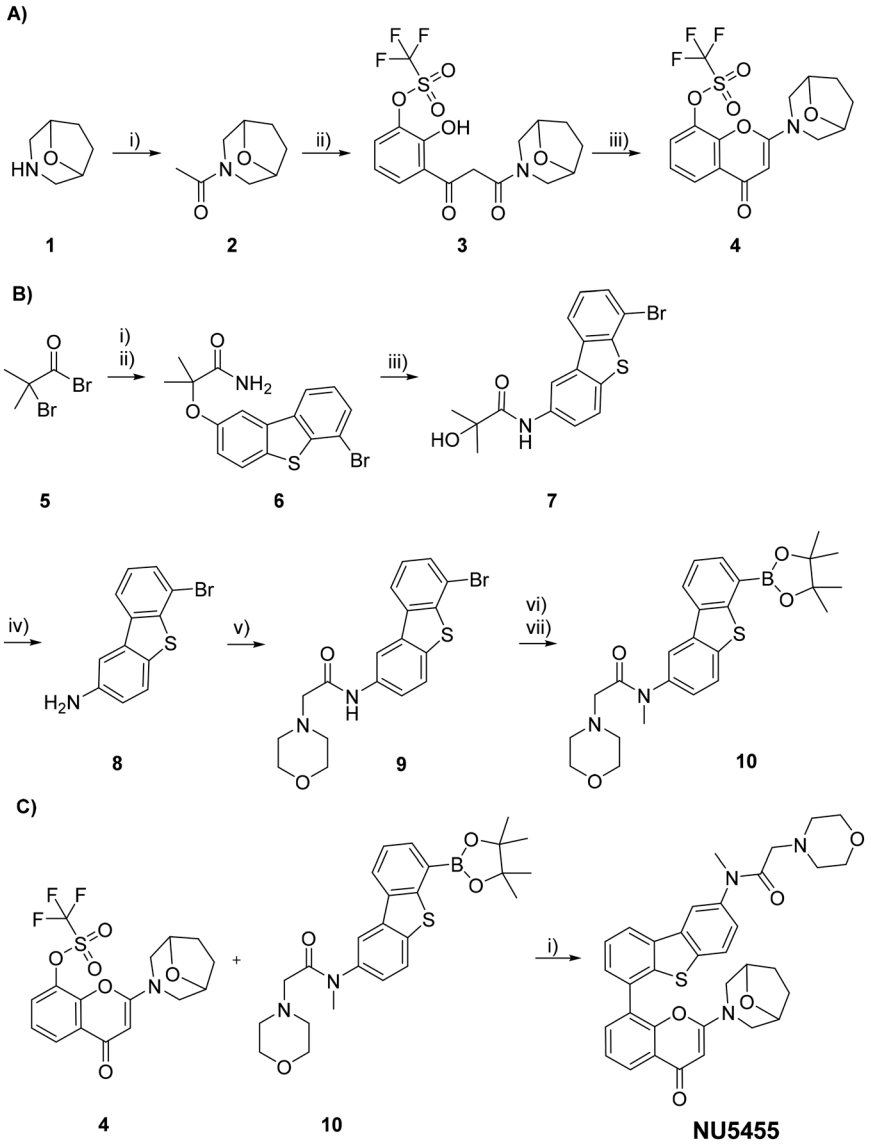

Scheme 1 Synthetic route to NU5455. A) Synthesis of intermediate **4**: i) Ac_2O, MP-carbonate, DIPEA, THF, N_2, rt, 18 h, quant; ii) ^{n}BuLi, DIPEA, THF, N_2, −70 °C, 30 min, then addition of **2**, −70 °C, 30 min, then addition of methyl 2-hydroxy-3-(trifluoromethylsulfonyloxy)benzoate, −77 °C, 2 h, crude; iii) Tf_2O, DCM, N_2, 0 °C, 5 min then rt, 18 h, 9%; B) synthesis of intermediate **10**: i) ammonium hydroxide, H_2O, 0–5 °C, 1 h, 64%; ii) 6-bromodibenzothiophen-2-ol, NaH, 1,4-dioxane, rt, 15 min, then addition of **5**, 100 °C, 40 h, 45%; iii) NaH, DMF, DMPU, N_2, 110 °C, 4 h; iv) HCl aq., EtOH, 100 °C, 18 h, 85%; v) chloroacetyl chloride, TEA, DMA, rt, 50 min then morpholine, 3 h, 68%; vi) sodium bis(trimethylsilyl)amide, THF, N_2, 0 °C, 30 min, iodomethane, rt, 20 min, 91%; vii) B_2pin_2, Pd(dppf)Cl_2, KOAc, 1,4-dioxane, N_2, 110 °C, 3 d, 87%. C) Synthesis of NU5455: i) Pd(PPh_3)$_4$, Na_2CO_2, 1,4-dioxane, N_2, reflux, 4 h, 15% (WO2010/136778).[48]

6-bromodibenzothiophen-2-ol. Migration of the amide on **6** in the presence of sodium hydride results in the displacement of the ether elegantly forms the amide **7** for subsequent deprotection to the free amine. Amide coupling with chloroacetyl chloride followed by methylation of the amide and a Miyaura borylation finalises the synthesis of intermediate **10**. The synthesis is highly efficient overall with high yields and short reaction duration with the exception of step iii in the synthesis of **3** and the finalising coupling which afford slightly lower yields.[48]

Human breast cancer cell lines were treated with NU5455 in combination with IR and it was shown to have a greater cell-killing effect in proliferating MCF7 cells.[49] Unfortunately, this response varied when explored in different cell types *in vitro*. Whereas NU5455 in combination with doxorubicin increased efficacy *in vivo*, suggesting therapeutic potential for treatment of hepatocellular carcinoma, associated with high DNA-PK expression linked treatment resistance.[50]

Moreover, *in vivo* treatment of Balb/C nude mice bearing HAP-1 xenografts with NU5455 in combination with radiation inhibited DNA DSBs repair which was not evident in the HAP1 PRKDC-/- xenografts indicating the specificity of NU5455 for DNA-PK_{cs} targeting.[51] Significantly, the inhibitory effect was more pronounced in hypoxic cells suggesting

NU5455 may act as a radiosensitiser of chronically hypoxic cancer cells.

KU-0060648. In 2012, using homology modelling of the DNA-PK ATP-binding site, derived from PI3Kγ,[52] Newcastle and AstraZeneca researchers introduced water-solubilising substituents to yield KU-0060648, a dual DNA-PK/PI3K inhibitor (DNA-PK IC_{50} = 5 nM).[53]

The synthesis of KU-0060648 begins with an electrophilic substitution of dibenzothiophene (**11**) and is followed by a nitration and triflation to afford **13** (Scheme 2). A Miyaura borylation affords **14** for the subsequent Suzuki coupling which yields the chromen-4-one **15**. The nitro group of **15** is reduced to form the corresponding free amine **16** which undergoes acylation with 1-ethylpiperazine in the finalising step to afford KU-0060648.

KU-0060648 effectively potentiated IR-induced and topoisomerase II poison-induced cytotoxicity, achieved dose-modification ratios up to 13 *in vitro* and displayed improved PK stability and solubility, low hERG inhibition, minimal CYP450 interaction and *in vivo* efficacy in xenograft tumour models.[25,53]

The balanced pharmacological profile of KU-0060648 has made it a benchmark for dual-target PIKK inhibitors and an invaluable tool for understanding DNA-PK's dual roles in DNA repair and oncogenic signalling. However, given the role PI3Kα plays in cardioprotection, the activity KU-0060648 displays against PI3Kα is preferably avoided in DNA-PK inhibitors.[54] Comparatively, the analogue NU5455 has a selectivity margin of 228-fold for DNA-PK_{cs} *versus* PI3Kα, hence Newcastle University shifted focus to the preclinical assessment of NU5455.

DA-143. Following the elucidation of NU7441 bound to DNA-PK_{cs} by Blundell *et al.*,[43] in 2024, Burdine *et al.* pursued modifications to the dibenzothiophene group, given its non-essential binding interactions, to improve the overall solubility of the compound.[56] Introduction of the pyrrolidine group provides both, metabolic stability, with the expectation of circumventing *N*-dealkylation, as well as being a readily ionisable group with a pK_a range of 9–11 capable of enhanced solubility (Fig. 3). DA-143 demonstrated comparable inhibition of kinase activity to NU7441 (IC_{50} = 2.5 nM) and sensitised cancer cells to doxorubicin without a notable reduction in selectivity against PI3K. Furthermore, DA-143 was shown to diminish autophosphorylation of DNA-PK_{cs} and other downstream substrates in the Jurkat T-cell line. Critically, both DA-143 and NU7441 were shown to reduce proliferation of CD4 and CD8 T cells as a consequence of down-regulated expression of IL-2 suggesting modulating DNA-PK_{cs} activity may have clinical value in the setting of autoimmune disorders.

The synthetic route towards DA-143 begins with 1-(3-bromo-2-hydroxyphenyl)ethan-1-one **17** and *N*,*N*-dimethylformamide dimethyl acetal (DMF-DMA) to yield 1-(3-bromo-2-hydroxyphenyl)-3-(dimethylamino)prop-2-en-1-one, followed by ring closure to chromenone **18.** This was then reacted with iodine and triazole to give **19**, followed by nucleophilic substitution and a Miyaura borylation cross-coupling to give **20** (Scheme 3A). 4-Bromodibenzo[*b*,*d*]thiophene **21** was reacted with iodine and iodobenzene diacetate to give **22.** Suzuki coupling of **22** with the corresponding boronic ester afforded dibenzothiophene **23** (Scheme 3B). A final Suzuki–Miyaura coupling between boronic ester **20** and dibenzothiophene **23** yielded DA-143 (Scheme 3C).

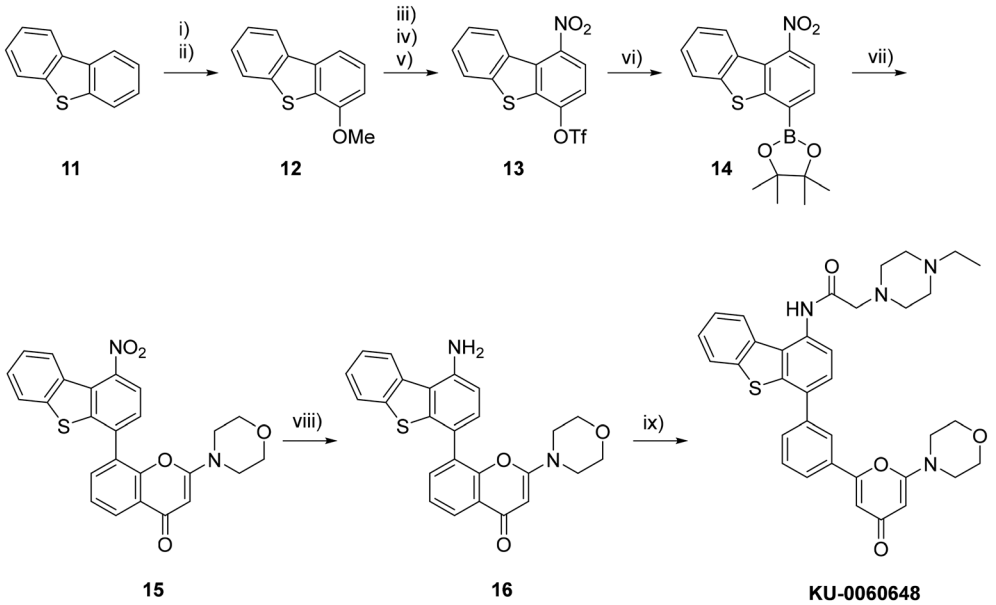

Scheme 2 Synthesis of KU-0060648: i) *n*-BuLi, THF, reflux then MeMgBr, O_2, 25 °C, 39%; ii) MeI, K_2CO_3, acetone, reflux, 96%; iii) HNO_3, AcOH, 25 °C, 99%; iv) pyridine hydrochloride, 150 °C, 41%; v) Tf_2O, NEt_3, DCM, 0 °C, 98%; vi) B_2pin_2, KOAc, $PdCl_2$(dppf), dppf, 1,4-dioxane, 95 °C, 66%; vii) 2-morpholino-4-oxo-4*H*-chromen-8-yl trifluoromethanesulfonate, $PdCl_2$(dppf), Cs_2CO_3, THF, 85 °C, 46%; viii) Zn, AcOH, 25 °C, 95%; ix) 1-ethylpiperazine, chloroacetyl chloride, NEt_3, DMA, rt, 95%.[55]

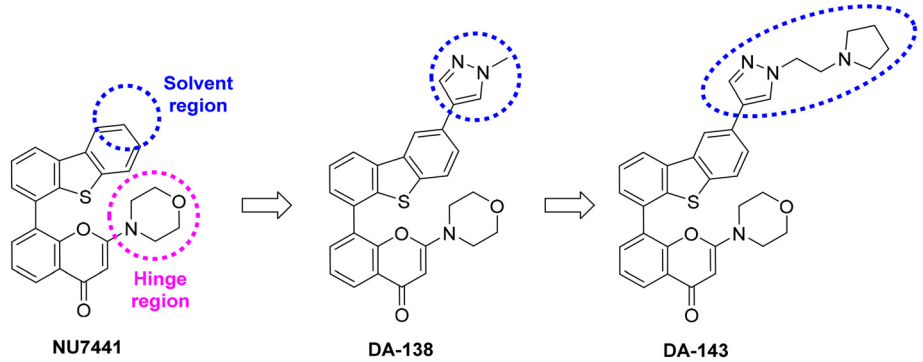

Fig. 3 SAR optimisation of DA-143.

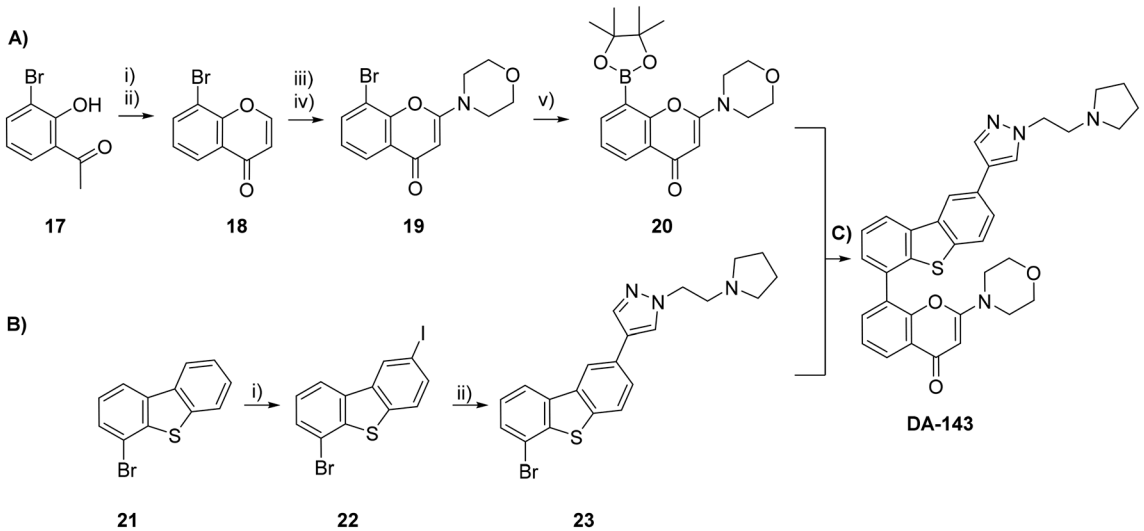

Scheme 3 Synthetic route DA-143. A) Synthesis of intermediate **20**: i) DMF acetal, DMF, 75 °C, 100%; ii) DCM, HCl, reflux, 90%; iii) triazole, iodine, K_2CO_3, DMF, 80 °C, 70%; iv) morpholine, K_2CO_3, DMF, 80 °C, 70%; v) bis(pinacolato)diboron, KOAc, $Pd(dppf)Cl_2$, 1,4-dioxane, 90 °C, 100%. B) Synthesis of intermediate **23**: i) iodine, iodobenzene diacetate, Ac_2O, AcOH, H_2SO_4, 45%; ii) 1-(2-(pyrrolidin-1-yl)ethyl)-4-(4,4,5,5-tetramethyl-1,3,2-dioxaborolan-2-yl)-1*H*-pyrazole, Na_2CO_3, $Pd(dppf)Cl_2$, 5 : 1 DMF : H_2O, 80 °C, 31%. C) Synthesis of DA-143: i) of 2-morpholino-8-(4,4,5,5-tetramethyl-1,3,2-dioxaborolan-2-yl)-4*H*-chromen-4-one, 4-(6-bromodibenzo[*b*,*d*]thiophen-2-yl)-1-(2-(pyrrolidin-1-yl)ethyl)-1*H*-pyrazole, K_2CO_3, $Pd(PPh_3)_4$, 1,4-dioxane, 90 °C, 32%.

The course of DNA-PK inhibitor development thus far illustrates the development of PIKK-targeted medicinal chemistry. Wortmannin established the concept of kinase-dependent radiosensitisation; KU-0060648 refined the pharmacophore toward selective, drug-like inhibitors; phenol-related IC compounds achieved potency with low toxicity and vanillin derivatives underscored the potential of covalent, fragment-based approaches. However, the emergence of next-generation inhibitors, such as M3814 and VX-984, marked a pivotal transition from chemical biology to therapeutic reality.

Next generation inhibitors

M3814. M3814 (also known as peposertib and nedisertib) is a potent, selective and orally bioavailable DNA-PK inhibitor.[57] Time-resolved FRET (TR-FRET) dose–response studies against a panel of 284 kinases revealed M3814 only inhibited the four class I PI3Ks (α, β, δ, γ), ATM, ATR and mTOR more than 50% at 1 μM.[58] M3814 was selective for DNA-PK_{cs} with ≥100-fold selectivity against the other PI3Ks and >1000-fold selectivity against ATR, ATM and mTOR.[58] With an IC_{50} of 0.6 nM in 10 μM ATP and 20 nM in 1 mM ATP, M3814 was confirmed to bind in the ATP binding site.[58] By Western blot analysis and ELISA assay, M3814 was also found to inhibit DNA-PK autophosphorylation on Ser2056 in a number of cell lines, suppressing NHEJ repair as this is a key residue for DNA-PK activation. In preclinical studies, M3814 showed limited efficacy as a monotherapy, but demonstrated a strong synergy with IR and DSB-inducing chemotherapeutics, significantly enhancing growth inhibition in multiple cell lines and human xenograft models. The enhanced growth inhibition observed in cell lines with elevated DNA-PK activity, together with increased synergy with DSB-inducing agents, supports inhibition of DNA-PK autophosphorylation as the primary mechanism of action of

M3814.[59] Preclinical studies also revealed that M3814 displayed some normal tissue toxicity. In mice, concurrent treatment of IR and temozolomide had no significant effect on weight, whereas combined therapy with M3814 resulted in a 15–20% drop in weight 8–9 days after the third dose of radiation. The mouse oral mucosa displayed significant mucositis in those treated with M3814 and IR, as compared to IR alone and control treatments, which shows the potential of M3814 to induce normal tissue toxicity.[60]

Structural analysis *via* cryo-electron microscopy (cryo-EM) revealed that the quinazoline and morpholine moieties point into the deepest hydrophobic pocket, as also seen in NU7441.[6,61] The chloro-fluorobenzene rotates −60° to point towards the N-lobe and the remaining pyridazine rotates to be almost parallel with the quinazoline, stabilising the interaction.[61] The sub-nanomolar potency and high selectivity of M3814 over closely related kinases may be the result of the drug exploiting these stabilising interactions within the ATP binding pocket, providing an advantage over previous treatments.

Notably, M3814 is one of three DNA-PK inhibitors to have reached phase II clinical trials, alongside AZD7648 and CC-115, and has been involved in 16 trials as of the writing of this review. In a first-in-human phase I study in patients with advanced solid tumours (NCT02316197), M3814 was well tolerated, with a recommended phase II dose (RP2D) of 400 mg twice daily (BID) established, but no maximum tolerated dose determined (MTD).[62] Pharmacodynamic (PD) analyses confirmed *in vivo* target engagement, displaying a decrease in phosphorylated DNA-PK on Ser2056 (p-DNA-PK) relative to total DNA-PK, measured by blood test before, 3 hours, and 6 hours after administration. As well as time-dependent, concentration-dependent p-DNA-PK inhibition could be observed with an approximate IC_{50} of 200 ng mL^{-1} established. In terms of efficacy, disease stabilisation was observed in 39% of patients, with no partial or complete response observed. This is consistent with M3814's mechanism as a sensitiser, rather than a cytotoxic agent.[62] In a different phase Ia/Ib trial (NCT02516813), M3814 was investigated in combination with IR but significant dose-limiting toxicities (DLTs) were observed, including grade 3 mucositis and grade 3 odynophagia toxicity. Other adverse effects included rash and radiation skin injury, highlighting the difficulty in selectively sensitising tumour tissue over normal tissue.[63,64] This may highlight a potential difficulty in inhibiting DNA-PK in general due to its involvement in multiple cellular pathways.

CC-115. In 2015, Celgene Corporation published the identification of CC-115, a dual inhibitor of kinases mTOR and DNA-PK_{cs}.[65] Initial investigations focused solely on the identification of an mTOR kinase inhibitor, *via* synthesis of a 1,6-substituted-imidazo[4,5-*b*]pyrazin-2-one series. Identification of CC214-1 was a promising hit, despite poor oral bioavailability, for SAR optimisation. Modifications around the imidazo-ring core including C6/7 substitutions and ring expansion were trialled leading to a triazole subseries in which CC-115 was identified (Fig. 4).[65] A screening of CC-115 against PI3K related kinases identified 65-fold selectivity for DNA-PK_{cs} with a determined IC_{50} of 13 nM (equipotent with its mTOR activity).[66] The elegantly simple and high yielding synthesis of CC-115 is achieved through a convergent synthetic route combining two intermediates, **25** and **27**, *via* a Suzuki–Miyaura coupling to form the complex **28** followed by a THF deprotection (Scheme 4). Synthesis of intermediate **25** is achieved by an intramolecular cyclisation of pyrazine **24** with ethanamine hydrochloride under basic conditions. Additionally, synthesis of intermediate **27** is achieved by Miyaura borylation of intermediate **26**.

In 2019, CC-115 underwent phase I clinical trials (NCT01353625) and 118 patients were treated with CC-115 for cancers including gastrointestinal, sarcoma, breast and lung *etc.*[67] As of 2023, CC-115 underwent phase Ib during which the drug was used in combination with enzalutamide to treat men with metastatic castration-resistant prostate cancer.[68] Additionally, between 2017 and 2021, a phase II clinical trial (NCT02977780) was conducted in which 12 patients were treated with CC-115.[43] Unfortunately, significant toxicity was observed and CC-115 failed to improve progression-free survival.

VX-984. VX-984 (M9831) is a selective inhibitor of DNA-PK_{cs}, developed by Vertex Pharmaceuticals. While detailed SAR and structural data have not been publicly disclosed, the compound shows clear target engagement and radiosensitises multiple tumour models.[69–71] Mechanistically, VX-984 suppresses IR-induced phosphorylation events such as phosphorylation of RPA-Ser4/Ser8 by DNA-PK_{cs} and Ser2056 autophosphorylation, resulting in blockage of NHEJ and persistent DNA damage.[70]

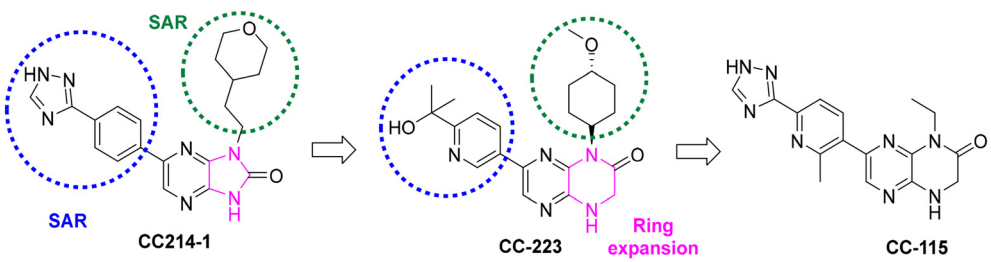

Fig. 4 SAR optimisation of 1,6-substituted-imidazo[4,5-*b*]pyrazin-2-one series, leading to CC-115.[65]

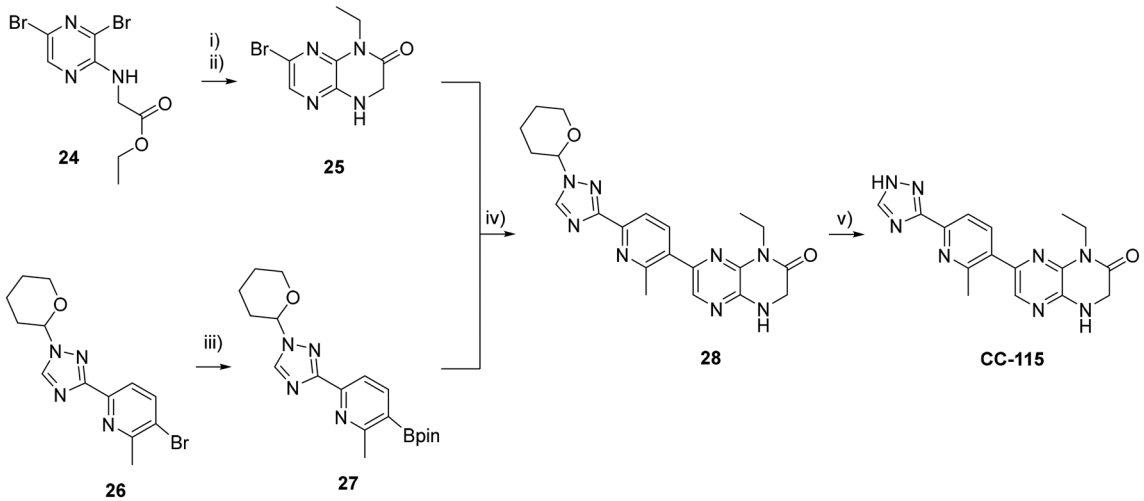

Scheme 4 Synthesis of CC-115: i) ethanamine hydrochloride, DIPEA, NMP, N_2, 105 °C, 14 h, 60% ii) AcOH, MeOH, 60 °C, 16 h, 75%; iii) B_2pin_2, Pd(dppf)Cl_2 (10%), potassium acetate, K_2CO_3, 1,4-dioxane, N_2, 90 °C, 2 h, 75%; iv) **28** at 40 °C, Pd(dppf)Cl_2 (5%), H_2O, N_2, 70 °C, 1 h, 57%; v) HCl, MeOH, 15-30 °C, 20 min, 81%.

Oral administration of VX-984 combined with radiotherapy enhances anti-tumour effects in glioblastoma models, demonstrating that the drug reaches pharmacologically relevant levels in the brain.[71] VX-984 advanced to a first-in-human phase I study (NCT02644278) as a monotherapy and in combination with pegylated liposomal doxorubicin (PLD) in advanced solid tumours. One review indicates that the trial is complete, but detailed results and progression to later-phase development have not been publicly disclosed.[72] A synthesis for VX-984 has been disclosed and is lengthy at 17 steps, though it is convergent and features a late-stage cross-coupling along with an asymmetric hydrogenation to set the (*S*) stereocentre (Scheme 5).[73] Notably, the deuterium atoms were incorporated as a strategy to overcome metabolism by aldehyde oxidases (AOs).[74]

AZD7648. In the search for DNA-PK_{cs} inhibitors with selectivity over the PI3K family, particularly PI3Kα, Goldberg *et al.* at AstraZeneca reported a high-throughput screening campaign of approximately 500 000 compounds from the AstraZeneca corporate collection against both targets. This identified a 7,9-dihydro-8*H*-purin-8-one core as a viable starting point. Subsequent structure–activity relationship (SAR) optimisation led to the discovery of AZD7648, a highly potent and selective DNA-PK_{cs} inhibitor (Fig. 5).[76,77]

AZD7648 was well optimised, achieving both, sub-nanomolar potency and selectivity over class I PI3Ks (>100-fold over PI3Kα/β/δ; 73-fold over PI3Kγ at 1 μM).[75] This *in vitro* potency translated well into cellular activity, with the IC_{50} of Ser2056 autophosphorylation, a marker of DNA-PK activation, being 91.3 nM.[6,76] These data support AZD7648 as one of the most potent and selective DNA-PK inhibitors reported to date.

Recent cryo-EM studies of the AZD7648–DNA-PK_{cs} complex have provided the first direct structural insight into inhibitor binding in the absence of a crystal structure of DNA-PK_{cs} bound with an inhibitor.[61] The study revealed a conserved binding mode *versus* AZD7648 bound to PI3Kγ, with the methyl-triazolopyridine moiety engaging a deep hydrophobic pocket, analogous to the binding of NU7441 and M3814.[61] A DNA-PK_{cs}-specific Lys3753 interaction and a Trp3805 reorientation enabling π-stacking are proposed to contribute to AZD7648's enhanced affinity and selectivity for DNA-PK_{cs}.[61]

Preclinical and early clinical studies have also shown AZD7648 to be an effective radio- and chemosensitiser. In combination with ionising radiation or doxorubicin, AZD7648 significantly enhances tumour cell cytotoxicity, and further synergistic effects are observed when combined with the PARP inhibitor olaparib.[75] A first-in-human phase I/IIa open-label study (NCT03907969) has been conducted on patients with advanced cancers.[77] The study reported safety/tolerability data, but very limited antitumour activity with AZD7648 monotherapy and only one RECIST partial response in combination therapy. The unexpectedly high toxicity of AZD7648 in combination with PLD resulted in early termination of the study.

In *in vivo* colon cancer studies in nude mice, the enhanced anti-tumour effect of AZD7648 and IR was lost as compared to the immunocompetent, resulting in no complete tumour regression. This suggests that the enhanced activity of AZD7648 in combination with IR is due to an increased antitumour immune response. Further studies showed this to be $CD8^+$ T-cell-dependent. The combination of AZD7648 and radiotherapy reduced PD-1 and Lag-3 exhaustion factors, although $CD8^+$ T-cell frequency itself was not increased. In comparison, tumour growth was accelerated in the absence of $CD8^+$ T-cells in deletion studies, indicating that AZD7648 and IR treatment induces $CD8^+$ T-cell-dependent antitumour response.[22]

AZD7648 is synthesised *via* a neat 9-step convergent route (Scheme 6) in which the methyl-triazolopyridine fragment and the purinone core are synthesised separately, then coupled late-stage. The methyl-triazolopyridine **45** is built *via* formation of a hydroxy-formimidamide **44** which subsequently undergoes

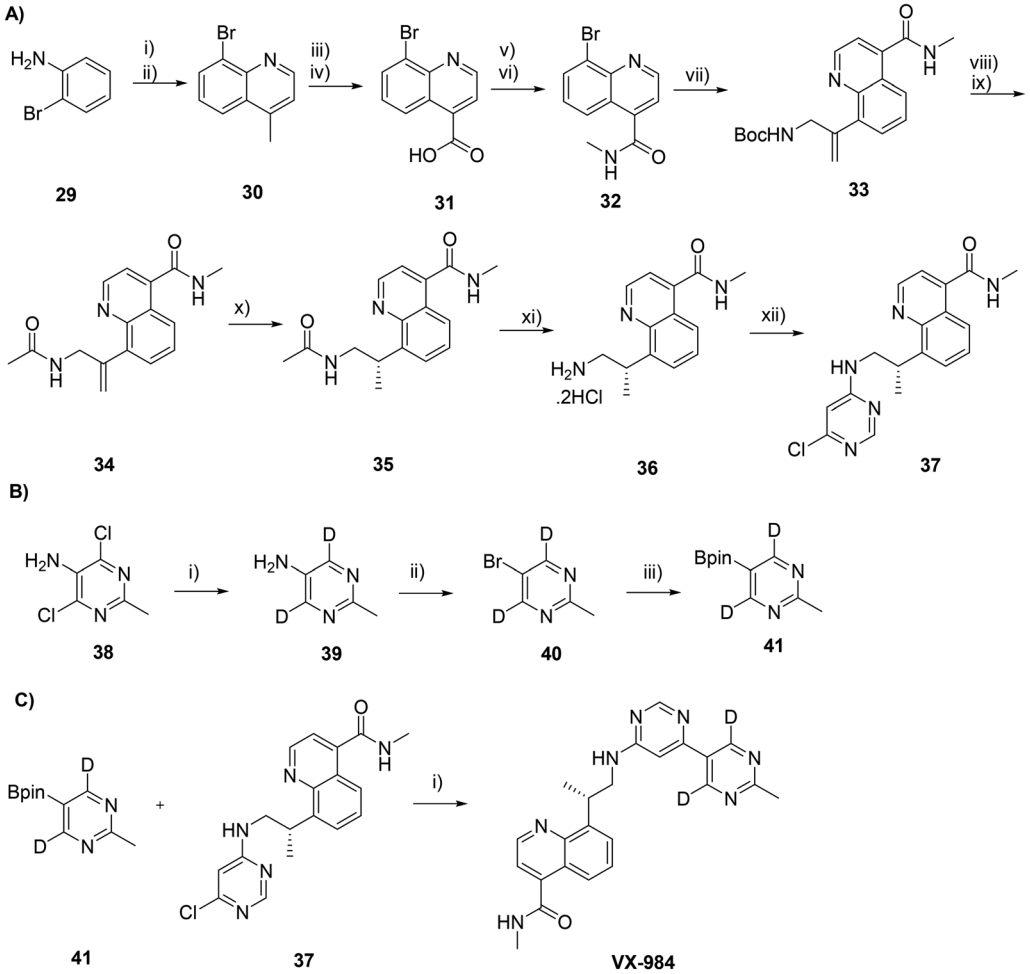

Scheme 5 Synthesis of VX-984: A) synthesis of intermediate **37**; i) But-3-en-2-one, $MeSO_3H$, AcOH, 90 °C; ii) NaOH (aq.); iii) SeO_2, 1,4-dioxane, H_2O, reflux, 30 min, 89%; iv) $NaClO_2$, NaH_2PO_4, THF, H_2O, 5 °C to rt, 2 h, 94%; v) $(COCl)_2$, DMF, DCM, 10 °C; vi) $MeNH_2$ (aq.), THF, 5 °C to rt, 16 h, 90% (over 2 steps); vii) *tert*-butyl (2-(4,4,5,5-tetramethyl-1,3,2-dioxaborolan-2-yl)allyl)carbamate, Pd(dppf)Cl_2/DCM, Na_2CO_3, 1,4-dioxane, H_2O, reflux, 16 h, 70%; viii) 5 M HCl in *i*PrOH, EtOH, 60 °C, 2 h; ix) Ac_2O, $NaHCO_3$, THF, H_2O, 0 °C to rt, 12 h, 62% (over 2 steps); x) H_2, 100 psi, Rh(COD)(*R*,*R*)-Et-DuPhos-OTf, MeOH, 50 °C, 14 h, 88%; xi) 6 M HCl, 60–70 °C, 4 days, 61%; xii) 4,6-dichloropyrimidine, Na_2CO_3, THF/H_2O, 66 °C, 2 h, 88%; B) synethesis of intermediate **41**: i) Pd (black), TEA, DCO_2D, $(D)_3COD$, 65%; ii) $CuBr_2$, $^tBuNO_2$, MeCN, rt, 1 h, 49%; iii) B_2pin_2, $PdCl_2[P(cy)_3]_2$, KOAc, 2-MeTHF, 100 °C, (72% purity, carried forward); C) synthesis of VX-984; i) 2 M Na_2CO_3, Silacat DPP Pd, 1,4-dioxane, 90 °C, 16 h, 28%.

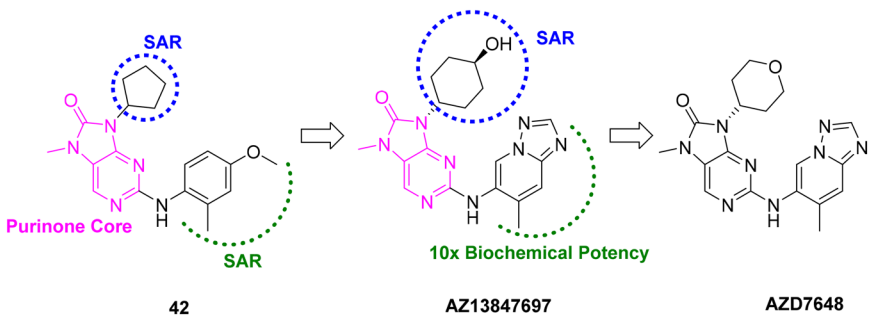

Fig. 5 SAR optimisation of initial screening hit **42** leading to the discovery of AZ13847697 and ultimately the lead compound AZD7648.

dehydration and cyclisation in the presence of TFAA and is finished by nitro reduction to the aniline **46**. The purinone core was assembled by S_NAr installation of the tetrahydropyran amine, ester hydrolysis, DPPA-mediated Curtius rearrangement to a urea and methylation. The two fragments are finally coupled in a Buchwald–Hartwig amination to give AZD7648.

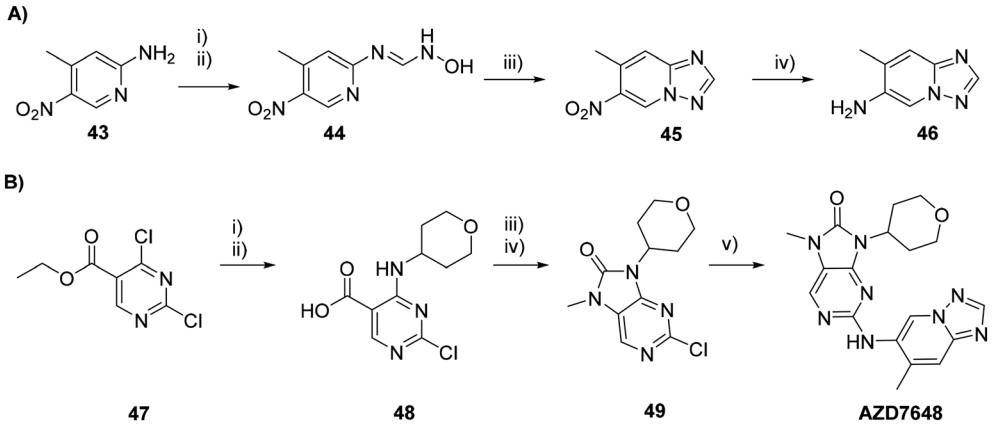

Scheme 6 Synthesis of AZD7648: A) synthesis of intermediate **46**; i) DMF-DMA, toluene, reflux, 2 h, 99%; (ii) $NH_2OH{\cdot}HCl$, MeOH, reflux, 1 h, 94%; (iii) TFAA, THF, 0 °C to rt, 18 h, 32%; (iv) Pd/C, NH_4HCO_2, EtOH, reflux, 2 h, 91%; B) synthesis of intermediate **49** and AZD7648; (i) K_2CO_3, tetrahydro-2*H*-pyran-4-amine hydrochloride, MeCN, rt, 16 h, 73%; (ii) LiOH, THF, H_2O, rt, 3 h, 92%; (iii) DPPA, NEt_3, DMA, 120 °C, 16 h, 70%; (iv) MeI, NaOH, H_2O, THF, rt, 16 h, 69%; (v) **46**, Brettphos Pd precat G3, Cs_2CO_3, 1,4-dioxane, 100 °C, 1.5 h, 54%.

Overall, the route benefits from a convergent design, reliable transformations and suitability for late-stage diversification.

D11. In early 2026, a new DNA-PK inhibitor, D11, the most potent in a series of novel heterotetracyclic DNA-PK inhibitors was discovered *via* scaffold hopping from AZD7648. The cryo-EM structure of AZD7648 bound to DNA-PK, elucidated by Liang *et al.*,[6] served as a starting point in their design strategy. By targeting the key π–π stacking interaction of the purinone core in AZD7648 with Trp3805 in DNA-PK, they initially designed two series of DNA-PK inhibitors *via* this scaffold hopping strategy. The representative compound out of both these series was DK1, possessing a 7,8-dihydropteridin-6(5*H*)-one core and an IC_{50} of 0.8 nM which performed better than AZD7648 (1.58 nM) in their assay. DK1 also showed strong synergistic antiproliferative activity in combination with doxorubicin in a range of cancer cell lines.[78] Further scaffold hopping modifications from this structure to a pentacyclic scaffold identified SK10, with a biochemical IC_{50} of 0.11 nM. *In vivo*, SK10 also displayed reasonable pharmacokinetic properties in colon cancer mouse models, including a moderate oral bioavailability (F = 31.8%), an improvement over their previous analogues, specifically DK1 (F = 20%).[79] D11 emerged from further optimisation using the scaffold-hopping strategy, moving from the heterotricyclic scaffold of SK10 to a heterotetracyclic scaffold. Importantly, D11 retains high biochemical potency (10.2 nM) and demonstrates significant selectivity for DNA-PK over all four class I PI3K isoforms (PI3Kα/β/δ/γ), with ATM being the only other kinase it inhibits more than 50% at 1 μM. This positions D11 as a possible dual DNA-PK–ATM inhibitor. Molecular modelling confirms that the scaffold engages in π–π stacking interactions with Trp3805, supporting the retained potency of D11. Consistent with its enzymatic potency, D11 demonstrated robust antiproliferative activity in a panel of cancer cell lines, including LoVo, Jurkat and HL-60 cells, with IC_{50} values as low as 1.6 μM.[80] Notably, D11 outperformed AZD7648 in the cellular assays, suggesting improved phenotypic activity as well as just target engagement. Mechanistically, D11 induced a concentration-dependent elevation in γH2AX (a biomarker for DSBs), confirming effective disruption of DSB repair.[81] This was accompanied by S-phase accumulation and inhibition of cancer cell migration, consistent with emerging roles of DNA-PK in metastasis-related signalling pathways. Pharmacokinetic evaluation in Sprague–Dawley rats showed D11 had a massively improved half-life ($t_{1/2}$ = 50 h, p.o.) compared to SK10 ($t_{1/2}$ = 2.0 h, p.o.) and improved oral bioavailability (F = 42.6%), suggesting favourable drug-likeness. These properties translated well into *in vivo* efficacy, with D11 achieving 72.9% tumour growth inhibition in a LoVo xenograft model at 50 mg kg^{-1} (p.o.). This efficacy was achieved without significant toxicity, evidenced by stable body weight, hinting at potential clinical efficacy. Beyond monotherapy, D11 demonstrated significant immunomodulatory potential. In a B16–F10 melanoma model, combination treatment with anti-PD-L1 antibody resulted in enhanced tumour suppression (growth inhibition = 69.6%) relative to either agent alone. This effect was associated with increased $CD8^+$ T-cell infiltration in tumour tissue, suggesting that DNA-PK inhibition augments antitumour immunity through enhanced DNA damage and neoantigen presentation.[80] The synthesis of D11 was achieved *via* a linear 8-step sequence, enabling efficient assembly of the heterotetracyclic core, followed by late-stage functionalisation with the terminal pyrimidine–piperazine (Scheme 7). Initial steps proceeded with high yield, such as S_NAr with tetrahydro-2*H*-pyran-4-amine to give **51**, subsequent reduction of the nitro group to give **52** and CDI-mediated cyclisation to give **53**. Thiourea formation to give **54** using P_2S_5 was achieved in good yield, as did the installation of the ethanolamine fragment to give **55**, and the subsequent cyclisation steps to give **57**. The final Suzuki–Miyaura coupling to give D11 proceeded only with modest yield. In summary, the route is robust and delivers the target compound in acceptable efficiency for discovery-phase studies. However, the reliance on linear synthesis, the use of harsh reagents and the diminished efficiency of the late-stage transformation limit scalability,

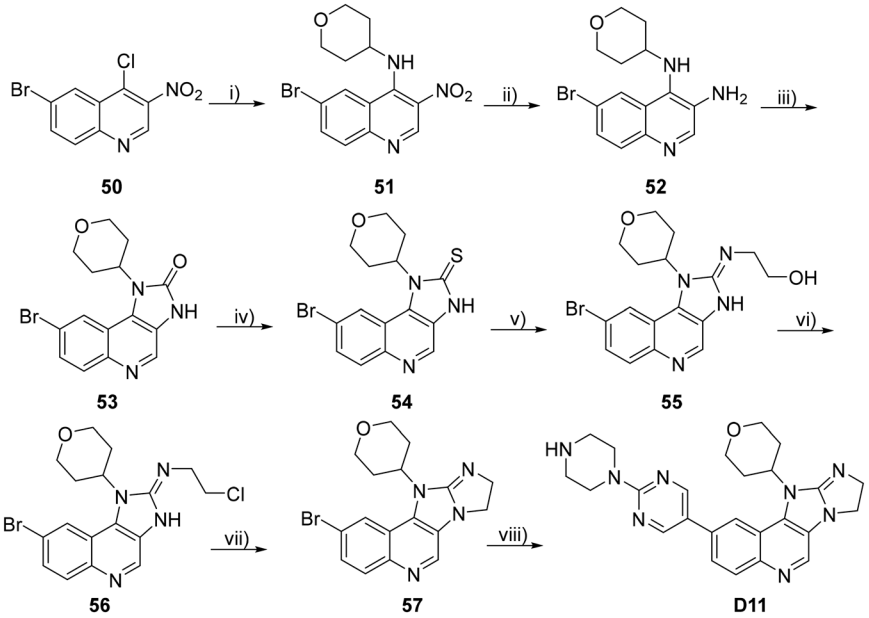

Scheme 7 Synthesis of D11. i) Tetrahydro-2*H*-pyran-4-amine, K_2CO_3, DMF, 25 °C, 12 h, 94%; ii) Fe powder, AcOH, 90 °C, 2 h, 90%; iii) CDI, DIPEA, DMF, 80 °C, 2 h, 88%; iv) P_2S_5, NEt_3, MeCN, 80 °C, 12 h, 82%; v) 2-aminoethan-1-ol, DMF, 70 °C, 2 h, 70%; vi) $SOCl_2$, DCM, 25 °C, 6 h, 95%; vii) DIPEA, KI, DMF, 100 °C, 12 h, 68%; viii) (2-(piperazin-1-yl)pyrimidin-5-yl)boronic acid, K_2CO_3, $Pd(PPh_3)_4$, 1,4-dioxane/H_2O (10 : 1), 90 °C, N_2, 10 h, 40–50%.

highlighting opportunities for future refinement. Overall, D11 is a potent DNA-PK inhibitor, with the potential for dual inhibition. It maintained strong target engagement, utilising the π–π stacking interaction with Trp3805, and possessing drug-like properties suitable enough for oral dosing, as well as the ability to boost immunotherapy. This positions D11 well for potential preclinical and clinical studies, after further investigations.

Separately, Hong *et al.*, reported the identification of a novel class of DNA-PK inhibitors based on an imidazo[4,5-*c*] pyridine-2-one scaffold also discovered through a scaffold hopping strategy from the purinone core of AZD7648.[82] Their lead, 'Compound **78**', exhibited a biochemical IC_{50} of approximately 8 nM and demonstrated selectivity over the other class I PI3Ks and mTOR.[82] In addition, 'Compound **78**' acted as an effective radiosensitiser *in vitro* and displayed high *in vivo* oral bioavailability (F = 88%), an improvement over other inhibitors developed by this strategy. This highlights the potential of exploring alternative heterocyclic cores to improve PK properties while retaining potency.

Efforts to further improve the PK profile of AZD7648-derived inhibitors were also reported by Liu *et al.* They employed a molecular docking approach to develop a series of analogues containing modifications around the triazolopyridine moiety to extend deeper into the hydrophobic pocket the group occupies.[83] Their lead, 'Compound **31t**' demonstrated an impressive IC_{50} of 0.1 nM with high selectivity over the other PI3Ks, together with favourable oral bioavailability (F = 85%). Furthermore, no significant changes in body weight were observed in mice treated with 'Compound **31t**' alone or in combination with paclitaxel, suggesting a favourable preliminary tolerability *in vivo*.[83]

BR101801. Boryung Pharmaceutical also pursued a DNA-PK inhibitor with improved solubility and pharmacokinetic properties. BR101801 was identified and shows comparable potency to NU7441, with an IC_{50} of 15 nM against DNA-PK_{cs}.[84] Significantly, BR101801 demonstrates a similar selectivity against PI3K family members and is effectively a triple inhibitor of PI3Kδ, PI3Kγ and DNA-PK. In 2020, BR10101 entered a phase I clinical trial (NCT04018248) which showed antitumour activity with a safe profile. As of 2025, BR101801 is in phase II clinical trials (NCT07180771) for the treatment of T-cell lymphoma.

The complete synthesis of BR101801 follows a 15-step synthetic route combining two key intermediates, **61** and **68** (Scheme 8). Synthesis of intermediate **61** begins with simultaneous Friedel Crafts and chlorination of pyrimidine-4,6-diol **58** followed by methylation and subsequent oxidation yields **59**. Pyrimidine **59** then undergoes S_NAr with *p*-methoxybenzylamine to afford pyrimidine **60** which then undergoes reaction with DMF-DMA, followed by intramolecular cyclisation in acidic conditions to afford **61**. In parallel, synthesis of intermediate **68** proceeds with the transformation of 2-chloro-6-methylbenzoic acid **62** to the corresponding acid chloride which undergoes reaction with aniline to form amide **63**. In the presence of ^{n}BuLi, the chiral auxillary (*S*)-3,5,9,9-tetramethyl-4,7-dioxo-2,8-dioxa-3,6-diazadecan-6-ide chloride undergoes nucleophilic attack from **63**. Under acidic conditions, **64** cyclises to form isoquinolinone **65**. Protection of the amine and subsequent chlorination yielded isoquinolinone **67**. Deprotection gave corresponding amine **68**. Finally, the two intermediates, **61** and **68**, undergo nucleophilic substitution and subsequent

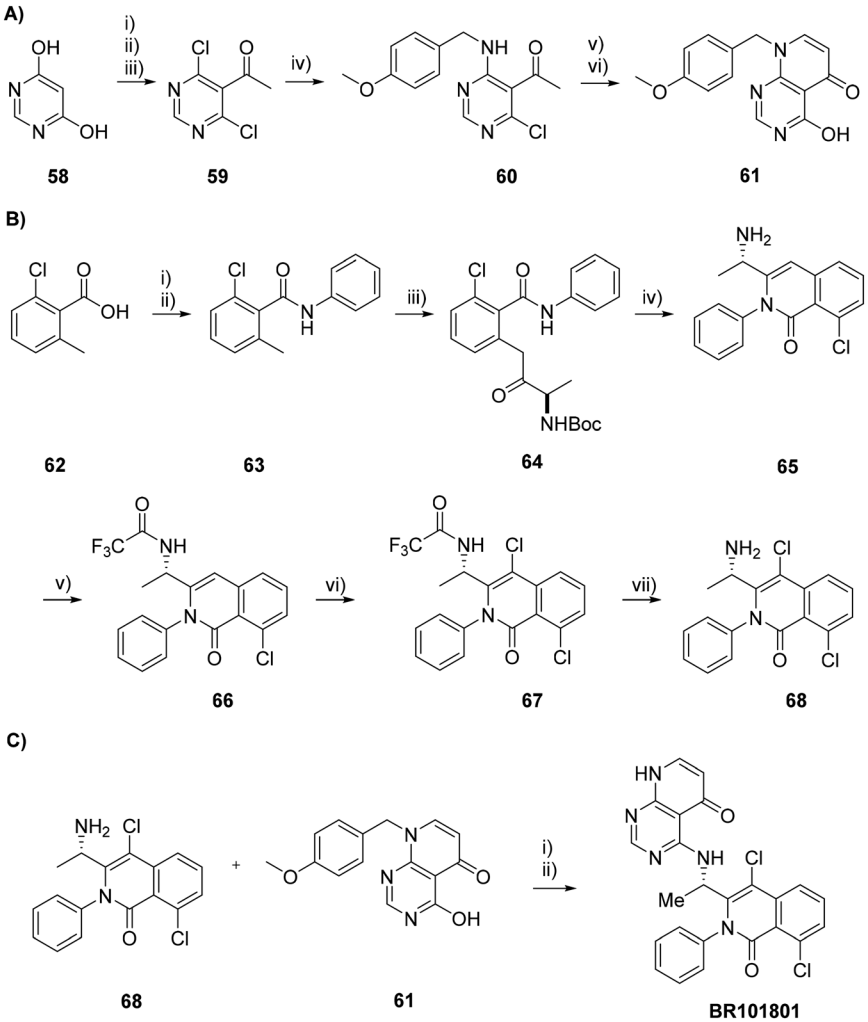

Scheme 8 Synthesis of BR101801. A) Synthesis of intermediate **47**: i) $POCl_3$, DMF, 0 °C for 1 h then rt, 30 min, 85%; ii) MeMgBr, THF, rt, 80%; iii) CrO_3, acetone, IPA, rt, 2 h, 85%; iv) *p*-methoxybenzylamine, DCM, 0 °C to rt; v) DMF-DMA, toluene, 100 °C, 3 h, 80%; vi) acetic acid, reflux, 3 h, 85%. B) Synthesis of intermediate **54**: i) oxalyl chloride, DCM, rt, 4 h, 100%; ii) aniline, TEA, DCM, 0 °C, 5 h, 87%; iii) ^{n}BuLi, THF, magnesium (*S*)-3,5,9,9-tetramethyl-4,7-dioxo-2,8-dioxa-3,6-diazadecan-6-ide chloride, −15 °C, 3 h, 86%,; iv) 12 N HCl, IPA, 65 °C then (*D*)-tartaric acid, MeOH, reflux, 2 h, 77%; v) TFAA, pyridine, DCM, 0 °C, 2 h, 97%; vi) NCS, MeCN, reflux, 4 h, 98%; vii) K_2CO_3, aq. MeOH, reflux, 12 h, 99%. C) Synthesis of BR101801: i) BOP/DBU, MeCN, 60 °C, 12 h, 50%; ii) TFA, MsCl, DCM, 70 °C, 10 h, 90%.[86,87]

deprotection to afford DNA-PK inhibitor BR101801.[85–87] Despite the synthetic route requiring multiple steps, the reactions are high yielding and efficient with reaction times no longer than 12 hours.

BAY-8400. In 2021, Siemeister and co-workers performed a screen of ATR inhibitors and identified the hit **55** with an IC_{50} of 153 nM and 10-fold DNA-PK selectivity (Fig. 6).[88] Resultant hit-to-lead optimisation explored a variety of scaffolds which ultimately led to the identification of BAY-8400 (IC_{50} = 81 nM). Initial SAR began with modification at the 8-position on the heterocyclic core and identified the *m*-difluoromethyl group of the 3-pyridyl residue to be beneficial effect in selectivity for DNA-PK over ATM. Further modifications were made to the heterocyclic core, swapping it for pyrazoloquinoline and imidazoquinoxaline scaffolds, however increased selectivity was not observed. Final optimisation focused on replacement of the THP group at the 1-position of the triazolo motif. Ring expansion, introduction of a double bond and exchange to a rigidified cyclic ether all resulted in an increased potency for both DNA-PK and PI3Kβ inhibition. As a result, BAY-8400 was identified with promising aqueous solubility and high

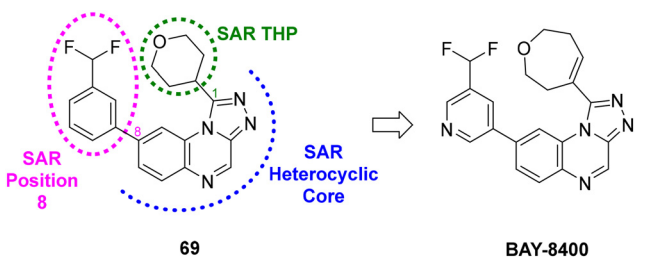

Fig. 6 Optimisation of BAY-8400 from initial hit **69** to the lead compound BAY-8400.

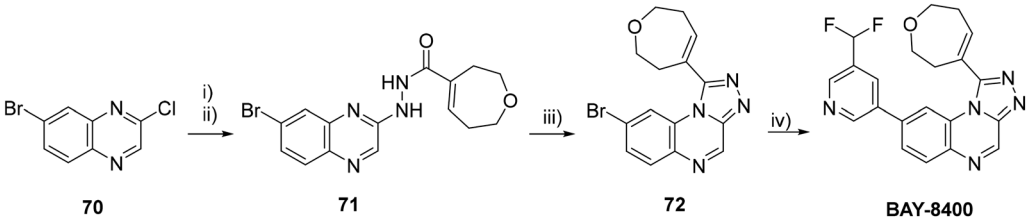

Scheme 9 Synthetic route to BAY-8400 i) H_2NNH_2, EtOH, 85 °C, 3 h, 74%; ii) 2,3,6,7-tetrahydrooxepine-4-carboxylic acid, HATU, *N*,*N*-diisopropylethylamine, DMF, rt, 1 h, 72%; iii) AcOH, 105 °C, 13 h, 63%; iv) 3-(difluoromethyl)-5-(4,4,5,5-tetramethyl-1,3,2-dioxaborolan-2-yl) pyridine, Pd(dppf)Cl_2, Na_2CO_3, 1,4-dioxane, 100 °C, 1.5 h, 90%.

selectivity over PI3K kinases such as ATM and mTOR. While single agent treatment with BAY-8400 failed to impact growth of *in vivo* LNCaP prostate cancer xenografts, combined treatment with a thorium-227 radionuclide labelled PSMA-targeting antibody demonstrated robust anti-tumour efficacy. Unfortunately, the pharmacokinetic properties of BAY-8400 are poor *in vitro*, including low metabolic stability and *in vivo* showed low oral bioavailability.

Synthesis of BAY-8400 is an elegant 4-step synthetic route which proceeds *via* S_NAr of quinoxaline **70** with hydrazine. This is followed by amide coupling with the appropriate carboxylic acid to afford hydrazide **71**. Under acidic conditions, hydrazide **71** undergoes ring closure to 1,2,4-triazole **72**. Finally, a Suzuki–Miyaura coupling affords the lead compound, BAY-8400 (Scheme 9). The optimised route is highly efficient with minimal steps and high yields.

XRD-0394. In 2024, Pharmaron collaborated with Xrad Therapeutics and Duke University School of Medicine to identify XRD-0394.[89] The dual ATM/DNA-PK inhibitor has an impressive IC_{50} of 0.89 nM against DNA-PK_{cs} and 0.39 nM against ATM and demonstrated 45-fold selectivity against PI3K and 100-fold against mTOR. A phase 1a clinical trial (NCT05002140) was completed in 2021, dosing patients with XRD-0394 in combination with radiotherapy and successfully provided rationale for further phase 1 clinical trials (NCT06829173).

Overall, the 14-step synthesis of XRD-0394 involves synthesis of two intermediates, **79** and **83** for a final Suzuki–Miyaura cross-coupling (Scheme 10). Synthesis of intermediate **79** begins with bromination of 2-amino-4-fluorobenzoic acid **73**, followed by chlorination of the amine to afford substituted benzene **74**. Introduction of the vinyl nitro group allowed for the subsequent ring closing to afford quinoline **75**. An Appel reaction is performed to form **76**, which reacts *via* S_NAr with methyl cyclobutanecarboxylate to form **77**. Reduction of the nitro group led to an intramolecular amide bond formation to form **78**, which was methylated to give intermediate **79**.

Synthesis of intermediate **83** begins with Boc protection of 2-(isopropylamino)ethan-1-ol (**80**) followed by S_NAr. The so-formed pyridine **81** undergoes mesylation followed by Boc deprotection to afford pyridine **82**. Lastly, a Miyaura borylation results in intermediate **83** (Scheme 10).

Conclusions

Over the past two decades, medicinal chemistry efforts have enabled DNA-PK inhibitors to evolve from early, non-selective and chemically unstable probes into highly potent, selective and orally bioavailable small molecules. Advances in structural biology, particularly cryo-EM, have provided critical insight into inhibitor binding modes, accelerating rational drug design. Although several next-generation inhibitors have progressed into clinical evaluation, challenges remain in achieving optimal selectivity, tolerability and therapeutic benefit in combination regimens involving radiotherapy or chemotherapeutics. Indeed, consistent with the application of PARP inhibitors in HR-defective cancers of the breast, ovary and prostate, it is likely that an emphasis on defining new susceptibility biomarkers to DNA-PK_{cs} blockade will propel these agents to becoming key therapeutics in appropriately sequenced treatment regimens. We anticipate the utility of high-throughput CRISPR and drug screening platforms, in combination with emerging data from DNA-PK inhibitor clinical trials data, will expedite rapid discovery and validation of these biomarkers for pronounced patient benefit.

The pivotal role of DNA-PK in NHEJ offers an exciting opportunity to develop more effective personalised combination strategies for DNA-PKIs in combination with current DDR-targeting agents. Indeed, including colon and prostate cancer, several synthetic–lethality relationships have been identified and experimentally validated between DNA-PK and genes involved in HDR including ATM and MSH3, respectively.[91] Moreover, recent drug screening approaches have demonstrated that loss of DNA-PK signalling enhanced sensitivity to both the tyrosine kinase inhibitor erlotinib and selective oestrogen receptor modulator raloxifene, supporting the rationale for defining and exploiting therapeutic vulnerabilities for improved DNA-PKI efficacy.[92] Crucially, the finding that mutations in MSH3 potentiated significant anti-tumour activity of single agent DNA-PKIs *in vivo* suggests identifying optimal susceptibility biomarkers may negate the requirement for in-parallel radio- or chemotherapy which would markedly expand the therapeutic window of these agents.

Outside of DDR, the pleiotropic roles of DNA-PK_{cs} as a key regulator of transcription, splicing and immune signalling further expands the repertoire of potential therapeutic

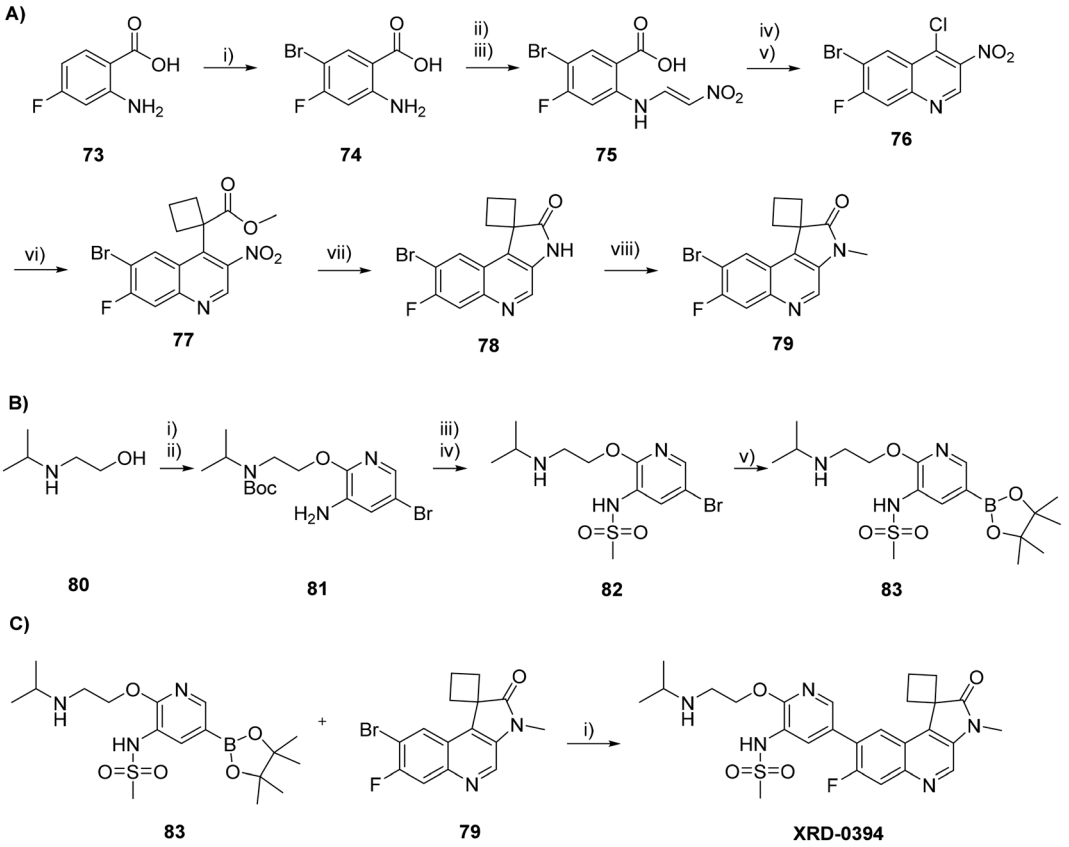

Scheme 10 Synthetic route to XRD-0394. A) Synthesis of intermediate **79**: i) NBS, DMF, −10 °C, 2 h, 76%; ii) 4 M HCl/1,4-dioxane, rt, 5 h, 96%; iii) CH_3NO_2, NaOH/H_2O, 25–80 °C, 20 min then HCl (aq.), rt, 16 h, 92%; iv) KOAc, Ac_2O, 40–140 °C, 45 min, 53%; v) $POCl_3$, TEA, 120 °C, 2 h, 91%; vi) methyl cyclobutanecarboxylate, LDA, THF, −78 °C, 2 h, 13%; vii) Fe, HOAc, rt, 18 h, 50%; viii) MeI, NaH, DMF, 0 °C, 30 min then rt, 40 min, 98%. B) Synthesis of intermediate **83**: i) Boc_2O, MeOH, 0 °C-rt, 2 h, 82%; ii) 5-bromo-2-chloropyridin-3-amine, NaH, THF, 0 °C-rt, 2 h, 71%; iii) Fe, HOAc, rt, 1 h, 86%; iv) MsCl, Py, rt, 16 h, 67%; v) 4 M HCl/1,4-dioxane, DCM, 0 °C-rt, 40 min, 50%; vi) B_2pin_2, Pd(dppf)Cl_2-DCM, KOAc, 1,4-dioxane, 90 °C, 16 h, 87%. C) Synthesis of XRD-0394: i) Pd$(PPh_3)_4$, Na_2CO_3, 1,4-dioxane, H_2O, 80 °C, 16 h, 82%.

opportunities for this important class of compounds. The control of numerous oncogenic transcription factors by DNA-PK, including AR, ERG and HIF-1, opens up exciting opportunities to formulate novel combination treatment paradigms involving DNA-PKIs and either (i) direct transcription factor-targeting drugs or (ii) compounds attenuating co-/epigenetic regulator activity. In prostate cancer, co-targeting DNA-PKI and AR with respective NU7441 and enzalutamide markedly down-regulated AR signalling,[93] and single agent DNA-PKI treatment diminished activity of pathogenic AR-*Vs*, ultimately providing a strong clinical rationale for application of DNA-PKIs in this disease.[19] Although interplay between DNA-PK and transcriptional co-regulators remains largely unexplored, DNA-PK has been shown to interact with and phosphorylate the histone acetyltransferase enzyme PCAF which is vital to elicit PCAF-mediated RPA1 acetylation and downstream nucleotide excision repair of UV-induced DNA adducts.[94,95] It is therefore important that future small molecule and CRISPR screening efforts to define new DNA-PKI-dependent vulnerabilities include epigenetic targets to exploit the involvement of DNA-PK in NHEJ, the wider DDR and transcriptional control.

From an immunobiology perspective, DNA-PK has received considerable interest as a regulator of both innate and adaptive immune responses. Given that immunotherapeutics have shown limited effectiveness across several cancer indications, developing new treatment regimens to enhance anti-tumour immunity is critical to fully realise the benefit of these agents. By enhancing cGAS signalling, DNA-PKIs have the capacity to activate innate immune signalling and priming of cytoxic T-cell populations. Crucially, in pre-clinical colon cancer studies *in vivo*, DNA-PK blockade was shown to enhance T-cell tumour infiltration, tumour cell killing and propagation of memory T cells to attenuate growth of re-challenged xenografts.[22] Whether this priming of cytotoxic T-cells is exclusively dependent on the cGAS pathway is currently unknown, but it is interesting to speculate that the role of DNA-PK in controlling pre-mRNA splicing may potentiate the formation of neo-antigens to boost anti-tumour immunity.[19] Future pre-clinical *in vivo* studies in immunocompetent hosts are therefore critical to understand interplay between DNA-PK and the immune system and test if

DNA-PK blockade can enhance the efficacy of current immunotherapeutics.

Ultimately, it is conceivable that with continued preclinical testing and biomarker discovery, better informed early phase combination trials will be realised in the short-term that could lead to DNA-PKIs playing a key role in personalised treatments across a wide spectrum of cancer indications.

Author contributions

E. W., J. R. R. H., S. J. H., L. G. and C. C. wrote the manuscript. All authors have given approval to the final version of the manuscript.

Conflicts of interest

There are no conflicts of interest to declare.

Data availability

No primary research results, software or code have been included, and no new data were generated or analysed as part of this review.

Acknowledgements

The authors gratefully acknowledge the EPRSC MoSMed CDT (EP/S022791/1, studentship award to E. W. and support for J. R. R. H.), Cancer Research Horizons and Newcastle University (studentship award to J. R. R. H.) and Cancer Research UK (DRCDDRPGMApr2020/100002, Newcastle Drug Discovery Unit Programme Grant, support for S. J. H.) for funding. Figures were created with https://www.BioRender.com.

References

1 D. C. van Gent, J. H. Hoeijmakers and R. Kanaar, *Nat. Rev. Genet.*, 2001, **2**, 196–206.
2 J. W. Harper and S. J. Elledge, *Mol. Cell*, 2007, **28**, 739–745.
3 J. San Filippo, P. Sung and H. Klein, *Annu. Rev. Biochem.*, 2008, **77**, 229–257.
4 M. R. Lieber, *Annu. Rev. Biochem.*, 2010, **79**, 181–211.
5 X. Yin, M. Liu, Y. Tian, J. Wang and Y. Xu, *Cell Res.*, 2017, **27**, 1341–1350.
6 S. Liang, S. E. Thomas, A. K. Chaplin, S. W. Hardwick, D. Y. Chirgadze and T. L. Blundell, *Nature*, 2022, **601**, 643–648.
7 H. H. Y. Chang, N. R. Pannunzio, N. Adachi and M. R. Lieber, *Nat. Rev. Mol. Cell Biol.*, 2017, **18**, 495–506.
8 S. Liang and T. L. Blundell, *Nat. Struct. Mol. Biol.*, 2023, **30**, 140–147.
9 T. A. Dobbs, J. A. Tainer and S. P. Lees-Miller, *DNA Repair*, 2010, **9**, 1307–1314.
10 J. P. Lees-Miller, A. Cobban, P. Katsonis, A. Bacolla, S. E. Tsutakawa, M. Hammel, K. Meek, D. W. Anderson, O. Lichtarge, J. A. Tainer and S. P. Lees-Miller, *Prog. Biophys. Mol. Biol.*, 2021, **163**, 87–108.
11 X. Yue, C. Bai, D. Xie, T. Ma and P.-K. Zhou, *Front. Genet.*, 2020, **11**, 607428.
12 M. Gellert, *Annu. Rev. Biochem.*, 2002, **71**, 101–132.
13 D. B. Roth, *Microbiol. Spectr.*, 2014, **2**, DOI: 10.1128/microbiolspec.mdna3-0041-2014.
14 D. G. Schatz and P. C. Swanson, *Annu. Rev. Genet.*, 2011, **45**, 167–202.
15 S. P. Jackson, J. J. MacDonald, S. Lees-Miller and R. Tjian, *Cell*, 1990, **63**, 155–165.
16 Y. Yang, H. Lu, C. Chen, Y. Lyu, R. N. Cole and G. L. Semenza, *Nat. Commun.*, 2022, **13**, 316.
17 J. C. Brenner, B. Ateeq, Y. Li, A. K. Yocum, Q. Cao, I. A. Asangani, S. Patel, X. Wang, H. Liang, J. Yu, N. Palanisamy, J. Siddiqui, W. Yan, X. Cao, R. Mehra, A. Sabolch, V. Basrur, R. J. Lonigro, J. Yang, S. A. Tomlins, C. A. Maher, K. S. J. Elenitoba-Johnson, M. Hussain, N. M. Navone, K. J. Pienta, S. Varambally, F. Y. Feng and A. M. Chinnaiyan, *Cancer Cell*, 2011, **19**, 664–678.
18 S. Liu, Y. Shao, Q. Wang, Y. Zhai and X. Li, *FEBS Open Bio*, 2019, **9**, 304–314.
19 B. Adamson, N. Brittain, L. Walker, R. Duncan, S. Luzzi, P. Rescigno, G. Smith, S. McGill, R. J. S. Burchmore, E. Willmore, I. Hickson, C. N. Robson, D. Bogdan, J. M. Jimenez-Vacas, A. Paschalis, J. Welti, W. Yuan, S. R. McCracken, R. Heer, A. Sharp, J. S. de Bono and L. Gaughan, *J. Clin. Invest.*, 2023, **133**, e169200.
20 E. Dylgjeri, V. Kothari, A. A. Shafi, G. Semenova, P. T. Gallagher, Y. F. Guan, A. Pang, J. F. Goodwin, S. Irani, J. J. McCann, A. C. Mandigo, S. Chand, C. M. McNair, I. Vasilevskaya, M. J. Schiewer, C. D. Lallas, P. A. McCue, L. G. Gomella, E. L. Seifert, J. S. Carroll, L. M. Butler, J. Holst, W. K. Kelly and K. E. Knudsen, *Clin. Cancer Res.*, 2022, **28**, 1446–1459.
21 X. Sun, T. Liu, J. Zhao, H. Xia, J. Xie, Y. Guo, L. Zhong, M. Li, Q. Yang, C. Peng, I. Rouvet, A. Belot, H.-B. Shu, P. Feng and J. Zhang, *Nat. Commun.*, 2020, **11**, 6182.
22 K. Nakamura, A. Karmokar, P. M. Farrington, N. H. James, A. Ramos-Montoya, S. J. Bickerton, G. D. Hughes, T. M. Illidge, E. B. Cadogan, B. R. Davies, S. J. Dovedi and V. Valge-Archer, *Clin. Cancer Res.*, 2021, **27**, 4353–4366.
23 F.-M. Hsu, S. Zhang and B. P. C. Chen, *Transl. Cancer Res.*, 2012, **1**, 22–34.
24 J. F. Goodwin, V. Kothari, J. M. Drake, S. Zhao, E. Dylgjeri, J. L. Dean, M. J. Schiewer, C. McNair, J. K. Jones, A. Aytes, M. S. Magee, A. E. Snook, Z. Zhu, R. B. Den, R. C. Birbe, L. G. Gomella, N. A. Graham, A. A. Vashisht, J. A. Wohlschlegel, T. G. Graeber, R. J. Karnes, M. Takhar, E. Davicioni, S. A. Tomlins, C. Abate-Shen, N. Sharifi, O. N. Witte, F. Y. Feng and K. E. Knudsen, *Cancer Cell*, 2015, **28**, 97–113.
25 J. M. Munck, M. A. Batey, Y. Zhao, H. Jenkins, C. J. Richardson, C. Cano, M. Tavecchio, J. Barbeau, J. Bardos, L. Cornell, R. J. Griffin, K. Menear, A. Slade, P. Thommes, N. M. B. Martin, D. R. Newell, G. C. M. Smith and N. J. Curtin, *Mol. Cancer Ther.*, 2012, **11**, 1789–1798.
26 A. Eriksson, R. Lewensoh, R. Larsson and A. Nilsson, *Anticancer Res.*, 2002, **22**, 1787–1793.

27 Å. Holgersson, A. Nilsson, R. Lewensohn and L. Kanter, *Exp. Mol. Pathol.*, 2004, **77**, 1–6.
28 G. Powis, R. Bonjouklian, M. M. Berggren, A. Gallegos, R. Abraham, C. Ashendel, L. Zalkow, W. F. Matter, J. Dodge and G. Grindey, *Cancer Res.*, 1994, **54**, 2419–2423.
29 R. A. Izzard, S. P. Jackson and G. C. M. Smith, *Cancer Res.*, 1999, **59**, 2581–2586.
30 M. P. Wymann, G. Bulgarelli-Leva, M. J. Zvelebil, L. Pirola, B. Vanhaesebroeck, M. D. Waterfield and G. Panayotou, *Mol. Cell. Biol.*, 1996, **16**, 1722–1733.
31 E. H. Walker, M. E. Pacold, O. Perisic, L. Stephens, P. T. Hawkins, M. P. Wymann and R. L. Williams, *Mol. Cell*, 2000, **6**, 909–919.
32 S. Boulton, S. Kyle, L. Yalçintepe and B. W. Durkacz, *Carcinogenesis*, 1996, **17**, 2285–2290.
33 C. J. Vlahos, W. F. Matter, K. Y. Hui and R. F. Brown, *J. Biol. Chem.*, 1994, **269**, 5241–5248.
34 R. J. Griffin, G. Fontana, B. T. Golding, S. Guiard, I. R. Hardcastle, J. J. J. Leahy, N. Martin, C. Richardson, L. Rigoreau, M. Stockley and G. C. M. Smith, *J. Med. Chem.*, 2005, **48**, 569–585.
35 Z. A. Knight, G. G. Chiang, P. J. Alaimo, D. M. Kenski, C. B. Ho, K. Coan, R. T. Abraham and K. M. Shokat, *Bioorg. Med. Chem.*, 2004, **12**, 4749–4759.
36 A. Kashishian, H. Douangpanya, D. Clark, S. T. Schlachter, C. T. Eary, J. G. Schiro, H. Huang, L. E. Burgess, E. A. Kesicki and J. Halbrook, *Mol. Cancer Ther.*, 2003, **2**, 1257–1264.
37 E. T. Shinohara, L. Geng, J. Tan, H. Chen, Y. Shir, E. Edwards, J. Halbrook, E. A. Kesicki, A. Kashishian and D. E. Hallahan, *Cancer Res.*, 2005, **65**, 4987–4992.
38 I. H. Ismail, S. Mårtensson, D. Moshinsky, A. Rice, C. Tang, A. Howlett, G. McMahon and O. Hammarsten, *Oncogene*, 2004, **23**, 873–882.
39 C. Cano, S. J. Harnor, E. Willmore and S. R. Wedge, Targeting DNA-PK as a Therapeutic Approach in Oncology, in *Targeting the DNA Damage Response for Anti-Cancer Therapy*, ed. J. Pollard and N. Curtin, Humana Press, New York, 2018, pp. 339–357.
40 S. J. Veuger, N. J. Curtin, C. J. Richardson, G. C. M. Smith and B. W. Durkacz, *Cancer Res.*, 2003, **63**, 6008–6015.
41 E. Willmore, S. De Caux, N. J. Sunter, M. J. Tilby, G. H. Jackson, C. A. Austin and B. W. Durkacz, *Blood*, 2004, **103**, 4659–4665.
42 O. R. Barbeau, C. Cano-Soumillac, R. J. Griffin, I. R. Hardcastle, G. C. M. Smith, C. Richardson, W. Clegg, R. W. Harrington and B. T. Golding, *Org. Biomol. Chem.*, 2007, **5**, 2670–2677.
43 S. Liang, S. E. Thomas, A. K. Chaplin, S. W. Hardwick, D. Y. Chirgadze and T. L. Blundell, *Nature*, 2022, **601**, 643–648.
44 F. S. Shaheen, P. Znojek, A. Fisher, M. Webster, R. Plummer, L. Gaughan, G. C. M. Smith, H. Y. Leung, N. J. Curtin and C. N. Robson, *PLoS One*, 2011, **6**, e20311.
45 W. M. Ciszewski, M. Tavecchio, J. Dastych and N. J. Curtin, *Breast Cancer Res. Treat.*, 2014, **143**, 47–55.
46 Y. Zhao, H. D. Thomas, M. A. Batey, I. G. Cowell, C. J. Richardson, R. J. Griffin, A. H. Calvert, D. R. Newell, G. C. M. Smith and N. J. Curtin, *Cancer Res.*, 2006, **66**, 5354–5362.
47 B. Adamson, N. Brittain, L. Walker, R. Duncan, S. Luzzi, P. Rescigno, G. Smith, S. McGill, R. J. S. Burchmore, E. Willmore, I. Hickson, C. N. Robson, D. Bogdan, J. M. Jimenez-Vacas, A. Paschalis, J. Welti, W. Yuan, S. R. McCracken, R. Heer, A. Sharp, J. S. de Bono and L. Gaughan, *J. Clin. Invest.*, 2023, **133**, e169200.
48 M. Frigerio, M. G. Hummerson, K. A. Menear, M. R. V. Finlay, E. J. Griffen, L. L. Ruston, J. J. Morris, A. K. T. Ting, B. T. Golding, R. J. Griffin, I. R. Hardcastle and S. Rodriguez-Aristegui, *WO Pat.*, WO2010/136778A1, 2010.
49 C. E. Willoughby, Y. Jiang, H. D. Thomas, E. Willmore, S. Kyle, A. Wittner, N. Phillips, Y. Zhao, S. J. Tudhope, L. Prendergast, G. Junge, L. M. Lourenco, M. R. V. Finlay, P. Turner, J. M. Munck, R. J. Griffin, T. Rennison, J. Pickles, C. Cano, D. R. Newell, H. L. Reeves, A. J. Ryan and S. R. Wedge, *J. Clin. Invest.*, 2020, **130**, 258–271.
50 L. Cornell, J. M. Munck, C. Alsinet, A. Villanueva, L. Ogle, C. E. Willoughby, D. Televantou, H. D. Thomas, J. Jackson, A. D. Burt, D. Newell, J. Rose, D. M. Manas, G. I. Shapiro, N. J. Curtin and H. L. Reeves, *Clin. Cancer Res.*, 2015, **21**, 925–933.
51 Y. Jiang, E. Willmore, S. R. Wedge and A. J. Ryan, *Mol. Cancer Ther.*, 2021, **20**, 1663–1671.
52 K. M. Clapham, T. Rennison, G. Jones, F. Craven, J. Bardos, B. T. Golding, R. J. Griffin, K. Haggerty, I. R. Hardcastle, P. Thommes, A. Ting and C. Cano, *Org. Biomol. Chem.*, 2012, **10**, 6747–6757.
53 C. Cano, K. Saravanan, C. Bailey, J. Bardos, N. J. Curtin, M. Frigerio, B. T. Golding, I. R. Hardcastle, M. G. Hummersone, K. A. Menear, D. R. Newell, C. J. Richardson, K. Shea, G. C. M. Smith, P. Thommes, A. Ting and R. J. Griffin, *J. Med. Chem.*, 2013, **56**, 6386–6401.
54 X. Rossello, J. A. Riquelme, Z. He, S. Taferner, B. Vanhaesebroeck, S. M. Davidson and D. M. Yellon, *Basic Res. Cardiol.*, 2017, **112**, 66.
55 C. Cano, K. Saravanan, C. Bailey, J. Bardos, N. J. Curtin, M. Frigerio, B. T. Golding, I. R. Hardcastle, M. G. Hummersone, K. A. Menear, D. R. Newell, C. J. Richardson, K. Shea, G. C. M. Smith, P. Thommes, A. Ting and R. J. Griffin, *J. Med. Chem.*, 2013, **56**, 6386–6401.
56 Z. J. Waldrip, B. Acharya, D. Armstrong, M. Hanafi, R. R. Rainwater, S. Amole, M. Fulmer, A. C. Azevedo-Pouly, A. Burns, L. Burdine, B. Frett and M. S. Burdine, *Sci. Rep.*, 2024, **14**, 19999.
57 F. T. Zenke, A. Zimmermann, C. Sirrenberg, H. Dahmen, L. Vassilev, U. Pehl, T. Fuchss and A. Blaukat, *Cancer Res.*, 2016, **76**, 1658.
58 F. T. Zenke, A. Zimmermann, C. Sirrenberg, H. Dahmen, V. Kirkin, U. Pehl, T. Grombacher, C. Wilm, T. Fuchss, C. Amendt, L. T. Vassilev and A. Blaukat, *Mol. Cancer Ther.*, 2020, **19**, 1091–1101.
59 S. B. Gordhandas, B. Manning-Geist, C. Henson, G. Iyer, G. J. Gardner, Y. Sonoda, K. N. Moore, C. Aghajanian, M. H. Chui and R. N. Grisham, *Sci. Rep.*, 2022, **12**, 974.

60 S. Dragojevic, J. Ji, P. K. Singh, M. A. Connors, R. W. Mutter, S. C. Lester, S. M. Talele, W. Zhang, B. L. Carlson, N. B. Remmes, S. S. Park, W. F. Elmquist, S. Krishnan, E. J. Tryggestad and J. N. Sarkaria, *Int. J. Radiat. Oncol., Biol., Phys.*, 2021, **111**, e54–e62.
61 Y. Matsumoto, *Int. J. Mol. Sci.*, 2022, **23**, 4264.
62 M. T. J. van Bussel, A. Awada, M. J. A. de Jonge, M. Mau-Sørensen, D. Nielsen, P. Schöffski, H. M. W. Verheul, B. Sarholz, K. Berghoff, S. El Bawab, M. Kuipers, L. Damstrup, I. Diaz-Padilla and J. H. M. Schellens, *Br. J. Cancer*, 2021, **124**, 728–735.
63 J. M. Brown, *Int. J. Radiat. Oncol., Biol., Phys.*, 2019, **103**, 1182–1183.
64 M. Mau-Sorensen, M. van Bussel, M. Kuipers, D. L. Nielsen, H. M. Verheul, P. Aftimos, M. J. A. de Jonge, B. van Triest, J. Falkenius, J. Debus, E. Troost, M. Samuels, B. Sarholz, V. Budach, S. Goel, G. Locatelli and P. F. Geertsen, *Ann. Oncol.*, 2018, **29**, viii654.
65 D. S. Mortensen, S. M. Perrin-Ninkovic, G. Shevlin, J. Elsner, J. Zhao, B. Whitefield, L. Tehrani, J. Sapienza, J. R. Riggs, J. S. Parnes, P. Papa, G. Packard, B. G. S. Lee, R. Harris, M. Correa, S. Bahmanyar, S. J. Richardson, S. X. Peng, J. Leisten, G. Khambatta, M. Hickman, J. C. Gamez, R. R. Bisonette, J. Apuy, B. E. Cathers, S. S. Canan, M. F. Moghaddam, H. K. Raymon, P. Worland, R. K. Narla, K. E. Fultz and S. Sankar, *J. Med. Chem.*, 2015, **58**, 5599–5608.
66 T. Tsuji, L. M. Sapinoso, T. Tran, B. Gaffney, L. Wong, S. Sankar, H. K. Raymon, D. S. Mortensen and S. Xu, *Oncotarget*, 2017, **8**, 74688–74702.
67 P. Munster, M. Mita, A. Mahipal, J. Nemunaitis, C. Massard, T. Mikkelsen, C. Cruz, L. Paz-Ares, M. Hidalgo, D. Rathkopf, G. Blumenschein, D. C. Smith, B. Eichhorst, T. Cloughesy, E. H. Filvaroff, S. Li, H. Raymon, H. de Haan, K. Hege and J. C. Bendell, *Cancer Manag. Res.*, 2019, **11**, 10463–10476.
68 J. L. Zhao, E. S. Antonarakis, H. H. Cheng, D. J. George, R. Aggarwal, E. Riedel, T. Sumiyoshi, J. D. Schonhoft, A. Anderson, N. Mao, S. Haywood, B. Decker, T. Curley, W. Abida, F. Y. Feng, K. Knudsen, B. Carver, M. E. Lacouture, A. W. Wyatt and D. Rathkopf, *Br. J. Cancer*, 2024, **130**, 53–62.
69 D. Boucher, R. Hoover, Y. Wang, Y. Gu, D. Newsome, P. Ford, C. Moody, V. Damagnez, R. Arimoto, S. Hillier, M. Wood, W. Markland, B. Eustace, K. Cottrell, M. Penney, B. Furey, K. Tanner, J. Maxwell and P. Charifson, *Cancer Res.*, 2016, **76**, 3716.
70 A. J. Khan, S. M. Misenko, A. Thandoni, D. Schiff, S. R. Jhawar, S. F. Bunting and B. G. Haffty, *Oncotarget*, 2018, **9**, 25833–25841.
71 C. R. Timme, B. H. Rath, J. W. O'Neill, K. Camphausen and P. J. Tofilon, *Mol. Cancer Ther.*, 2018, **17**, 1207–1216.
72 T. Zheng, C. Sun, C. Yun, H. Wang and X. Liu, *Cancers*, 2025, **17**, 2787.
73 P. S. Charifson, K. M. Cottrell, H. Deng, J. P. Duffy, H. Gao, S. Giroux, J. Green, K. L. Jackson, J. M. Kennedy, D. J. Lauffer, M. W. Ledeboer, P. Li, J. P. Maxwell, M. A. Morris, A. C. Pierce, N. D. Waal and J. Xu, *US Pat.*, US2013281431A1, 2013.
74 J. L. Koniarczyk, D. Hesk, A. Overgard, I. W. Davies and A. McNally, *J. Am. Chem. Soc.*, 2018, **140**, 1990–1993.
75 J. H. L. Fok, A. Ramos-Montoya, M. Vazquez-Chantada, P. W. G. Wijnhoven, V. Follia, N. James, P. M. Farrington, A. Karmokar, S. E. Willis, J. Cairns, J. Nikkilä, D. Beattie, G. M. Lamont, M. R. V. Finlay, J. Wilson, A. Smith, L. O. O'Connor, S. Ling, S. E. Fawell, M. J. O'Connor, S. J. Hollingsworth, E. Dean, F. W. Goldberg, B. R. Davies and E. B. Cadogan, *Nat. Commun.*, 2019, **10**, 5065.
76 F. W. Goldberg, M. R. V. Finlay, A. K. T. Ting, D. Beattie, G. M. Lamont, C. Fallan, G. L. Wrigley, M. Schimpl, M. R. Howard, B. Williamson, M. Vazquez-Chantada, D. G. Barratt, B. R. Davies, E. B. Cadogan, A. Ramos-Montoya and E. Dean, *J. Med. Chem.*, 2020, **63**, 3461–3471.
77 T. A. Yap, P. LoRusso, R. E. Miller, R. Kristeleit, A. G. Paulovich, S. McMorn, L. Oplustil O'Connor, B. Lombardi, P. Marco-Casanova, E. T. Gangl, B. Patel, M. J. O'Connor, E. Dean, R. Zviezdin and R. Plummer, *Br. J. Cancer*, 2025, **133**, 168–177.
78 Z. Ding, W. Pan, Y. Xiao, B. Cheng, G. Huang and J. Chen, *Eur. J. Med. Chem.*, 2022, **237**, 114401.
79 B. Cheng, Y. Shi, C. Shao, S. Wang, Z. Su, J. Liu, Y. Zhou, X. Fei, W. Pan, J. Chen, Y. Lu and J. Xiao, *J. Med. Chem.*, 2024, **67**, 6253–6267.
80 B. Guan, B. Cheng, S. Cheng, J.-J. Du and C. Wen, *J. Med. Chem.*, 2026, **69**, 4913–4931.
81 L. J. Kuo and L.-X. Yang, *In Vivo*, 2008, **22**, 305.
82 C. R. Hong, L. P. Liew, W. W. Wong, B. D. Dickson, G. Cheng, A. Shome, R. Airey, J. Jaiswal, B. Lipert, S. M. F. Jamieson, W. R. Wilson and M. P. Hay, *J. Med. Chem.*, 2024, **67**, 12366–12385.
83 K. Liu, X. Yuan, T. Yang, D. Deng, Y. Chen, M. Tang, C. Zhang, Y. Zou, S. Zhang, D. Li, M. Shi, Y. Guo, Y. Zhou, M. Zhao, Z. Yang and L. Chen, *J. Med. Chem.*, 2024, **67**, 245–271.
84 S. Wang, Y. N. Yoon, M. kwon Son, S. J. Kim, B. R. Lee, E. hee Yang, B. Jeon, S. H. Lee, T.-J. Kim, J.-S. Kim and J. H. Lee, *BMJ*, 2021, A630.
85 L. G. Hyeong, L. Hee-Jong, C. Heeyeong, P. W. Kyu, K. S. Hwan and C. J. Hwan, *WO Pat.*, WO2016204429A1, 2016.
86 B. Jeon, Y. J. Lee, J. Shin, M.-J. Choi, C.-E. Lee, M. K. Son, J. H. Park, B.-S. Kim, H. R. Kim, K. H. Jung, J.-H. Cha and S.-S. Hong, *Am. J. Cancer Res.*, 2023, **13**, 452–463.
87 L. G. Hyeong, L. Hee-Jong, C. Heeyeong, P. W. Kyu, K. S. Hwan and C. J. Hwan, *US Pat.*, US2018105527A1, 2018.
88 M. Berger, L. Wortmann, P. Buchgraber, U. Lücking, S. Zitzmann-Kolbe, A. M. Wengner, B. Bader, U. Bömer, H. Briem, K. Eis, H. Rehwinkel, F. Bartels, D. Moosmayer, U. Eberspächer, P. Lienau, S. Hammer, C. A. Schatz, Q. Wang, Q. Wang, D. Mumberg, C. F. Nising and G. Siemeister, *J. Med. Chem.*, 2021, **64**, 12723–12737.
89 T. M. Gilmer, C. H. Lai, K. Guo, K. Deland, K. A. Ashcraft, A. E. Stewart, Y. Wang, J. Fu, K. C. Wood, D. G. Kirsch and M. B. Kastan, *Mol. Cancer Ther.*, 2024, **23**, 751–765.
90 F. Chen, H. Zhao, C. Li, P. Li and Q. Zhang, *Cell Death Discovery*, 2022, **8**, 293.

91 E. Callén, M. Jankovic, N. Wong, S. Zha, H.-T. Chen, S. Difilippantonio, M. Di Virgilio, G. Heidkamp, F. W. Alt, A. Nussenzweig and M. Nussenzweig, *Mol. Cell*, 2009, **34**, 285–297.
92 D. Macak, P. Kanis and S. Riesenberg, *Nat. Commun.*, 2025, **16**, 11077.
93 E. Dylgjeri, C. McNair, J. F. Goodwin, H. K. Raymon, P. A. McCue, A. A. Shafi, B. E. Leiby, R. de Leeuw, V. Kothari, J. J. McCann, A. C. Mandigo, S. N. Chand, M. J. Schiewer, L. J. Brand, I. Vasilevskaya, N. Gordon, T. S. Laufer, L. G. Gomella, C. D. Lallas, E. J. Trabulsi, F. Y. Feng, E. H. Filvaroff, K. Hege, D. Rathkopf and K. E. Knudsen, *Clin. Cancer Res.*, 2019, **25**, 5623–5637.
94 N. A. Barlev, V. Poltoratsky, T. Owen-Hughes, C. Ying, L. Liu, J. L. Workman and S. L. Berger, *Mol. Cell. Biol.*, 1998, **18**, 1349–1358.
95 M. Zhao, R. Geng, X. Guo, R. Yuan, X. Zhou, Y. Zhong, Y. Huo, M. Zhou, Q. Shen, Y. Li, W. Zhu and J. Wang, *Cell Rep.*, 2017, **20**, 1997–2009.